

1 **Phenethylamine-producing gut bacteria induces diarrhea-predominant irritable bowel**  
2 **syndrome by increasing serotonin biosynthesis**

3 Lixiang Zhai <sup>1, +</sup>, Chunhua Huang <sup>1, 2, +</sup>, Ziwan Ning <sup>1, 2, +</sup>, Yijing Zhang <sup>2, +</sup>, Min Zhuang <sup>1</sup>,  
4 Wei Yang <sup>1</sup>, Xiaolei Wang <sup>3</sup>, Jingjing Wang <sup>4</sup>, Eric Lu Zhang <sup>4</sup>, Haitao Xiao <sup>5</sup>, Ling Zhao <sup>6</sup>,  
5 Yan Y. Lam <sup>1</sup>, Chi Fung Willis Chow<sup>7</sup>, Jiandong Huang <sup>3</sup>, Shuofeng Yuan<sup>8</sup>, Kui Ming Chan<sup>9</sup>,  
6 Hoi Leong Xavier Wong <sup>2, \*</sup>, Zhao-xiang Bian <sup>1, 2, \*</sup>

7 <sup>1</sup> Centre for Chinese Herbal Medicine Drug Development Limited, Hong Kong Baptist  
8 University, Hong Kong SAR, China;

9 <sup>2</sup> School of Chinese Medicine, Hong Kong Baptist University, Hong Kong SAR, China;

10 <sup>3</sup> School of Biomedical Sciences, Li Ka Shing Faculty of Medicine, University of Hong Kong,  
11 Hong Kong SAR, China;

12 <sup>4</sup> Department of Computer Science, Hong Kong Baptist University, Hong Kong SAR, China;

13 <sup>5</sup> School of Pharmaceutical Sciences, Health Science Center, Shenzhen University, Shenzhen,  
14 China;

15 <sup>6</sup> Academy of Integrative Medicine, Shanghai University of Traditional Chinese Medicine,  
16 Shanghai, China;

17 <sup>7</sup> Center for Systems Biology Dresden, Max Planck Institute for Molecular Cell and Biology,  
18 Dresden, Germany;

19 <sup>8</sup> State Key Laboratory of Emerging Infectious Diseases, Carol Yu Centre for Infection,  
20 Department of Microbiology, Li Ka Shing Faculty of Medicine, The University of Hong  
21 Kong, Hong Kong SAR, China;

22 <sup>9</sup> Department of Biomedical Sciences, City University of Hong Kong, Hong Kong SAR,  
23 China

24 <sup>+</sup> Co-first authors: Lixiang Zhai, Chunhua Huang, Ziwan Ning and Yijing Zhang

25 <sup>\*</sup> Correspondence:

26 Hoi Leong Xavier Wong, Ph.D. School of Chinese Medicine, Hong Kong Baptist University,  
27 Hong Kong SAR, China. E-mail: [xavierwong@hkbu.edu.hk](mailto:xavierwong@hkbu.edu.hk)

28 Zhao-Xiang Bian, MD, Ph.D. Centre for Chinese Herbal Medicine Drug Development  
29 Limited, Hong Kong Baptist University, Hong Kong SAR, China; School of Chinese

30 Medicine, Hong Kong Baptist University, Hong Kong SAR, China; E-mail:

31 [bxxiang@hkbu.edu.hk](mailto:bxxiang@hkbu.edu.hk);

## 32 **Summary**

33 Despite the strong association between gut microbial dysbiosis, serotonin (5-HT)  
34 dysregulation and diarrhea-predominant irritable bowel syndrome (IBS-D), the mechanism  
35 by which changes in the gut microbiota contribute to the pathogenesis of IBS-D, particularly  
36 the role of dysregulated 5-HT production, remains unclear. The present study identified  
37 *Ruminococcus gnavus* in the human gut microbiota as a key risk factor of IBS-D. *R. gnavus*  
38 was significantly enriched in IBS-D patients and exhibited positive correlation with serum 5-  
39 HT level and severity of diarrhea symptoms. We showed that *R. gnavus* induced diarrhea-like  
40 symptoms in mice by promoting microbial shunting of essential aromatic amino acids to  
41 aromatic trace amines including phenethylamine and tryptamine, thereby stimulating the  
42 biosynthesis of peripheral 5-HT, a potent stimulator for gastrointestinal transit. This study  
43 identify gut-microbial metabolism of dietary amino acids as a cause of IBS-D and lays a  
44 foundation for developing novel therapeutic target for the treatment of IBS-D.

## 45 **Keywords:**

46 Aromatic trace amines; Phenethylamine; Tryptamine; Serotonin; Gastrointestinal motility;  
47 Colonic secretion; Irritable bowel syndrome; Trace amine-associated receptor 1; Gut  
48 microbiota

## 49 **Running title:**

50 Phenethylamine induces diarrhea-predominant irritable bowel syndrome

## 51 **Abbreviations:**

5-Hydroxyindole acetic acid	5-HIAA
5-Hydroxytryptophan	5-HTP
Serotonin	5-HT
Calmodulin-dependent protein kinase II	CaMKII
Enterochromaffin cells	EC
Gastrointestinal	GI
3-Indole acetic acid	IAA
Irritable bowel syndrome	IBS
Diarrhea-predominant irritable bowel syndrome	IBS-D
Phenylacetic acid	PA
Phenethylamine	PEA

Phenylalanine	Phe
Cyclic AMP-dependent protein kinase	PKA
Trace amine-associated receptor 1	TAAR1
Tryptamine	TpA
Tryptophan hydroxylase 1	TPH1
Tryptophan	Trp

52

## 53 **Introduction**

54 Irritable bowel syndrome (IBS) is one of the most prevalent functional bowel disorders  
55 characterized by an array of gastrointestinal (GI) symptoms including abdominal pain,  
56 bloating, abdominal distention and bowel habit abnormalities (Sperber et al., 2017). IBS is  
57 associated with comorbid conditions that substantially reduce the quality of life, leading to a  
58 growing social and economic burden worldwide. Despite the high prevalence of IBS,  
59 treatment options for the management of IBS are limited (Van den Houte et al., 2020), and  
60 most therapeutic approaches can only relieve individual symptoms of IBS instead of curing  
61 it..

62 Serotonin (5-HT) is an important neurotransmitter synthesized from tryptophan by  
63 tryptophan decarboxylase 1 (TPH1) in intestinal enterochromaffin cells (ECs) and tryptophan  
64 decarboxylase 2 (TPH2) in enteric and central serotonergic neurons (Bellono et al., 2017). 5-  
65 HT released from EC cells in the GI tract modulates gut motility and hypersensitivity  
66 functions (Kendig and Grider, 2015). EC cell hyperplasia and increased 5-HT production are  
67 often observed in the colon of IBS patients, especially those with diarrhea-predominant IBS  
68 (IBS-D) (Dunlop et al., 2003; Thijssen et al., 2016). Increased production of peripheral 5-HT  
69 from intestinal EC cells can lead to intestinal symptoms in IBS-D (Wong et al., 2019).  
70 Therapeutic interventions targeting various 5-HT receptors have been shown to be effective  
71 in the management of IBS, but their therapeutic effects are hampered by adverse  
72 complications, such as ischemic colitis and severe constipation (Stasi et al., 2014). Therefore,  
73 an improved understanding of the mechanism underlying increased 5-HT production in IBS-  
74 D patients may pave the way for innovative therapeutic strategies against IBS-D.

75 Emerging evidence reveals that gut microbiota plays an important role in the  
76 pathophysiology of IBS. In alignment with other studies, our previous findings have reported  
77 significant changes in the structure of gut microbiota in patients with IBS, especially in IBS-  
78 D (Han et al., 2021; Jeffery et al., 2020; Zhao et al., 2020). Transplantation of fecal  
79 microbiota from IBS-D patients results in IBS-like symptoms including accelerated GI transit  
80 and intestinal barrier dysfunction in recipient germ-free mice (De Palma et al., 2017). Despite  
81 the strong association between gut dysbiosis and the pathogenesis of IBS, the mechanism by  
82 which changes in the gut microbiota contributes to the development of IBS remain unclear.

83 Gut microbiota is essential for the maintenance of homeostatic peripheral 5-HT levels in the  
84 host since serum 5-HT levels are remarkably reduced in germ-free mice (Reigstad et al., 2015;  
85 Yano et al., 2015). Moreover, gut microbial metabolites, such as secondary bile acids and  
86 short-chain fatty acids, stimulate peripheral 5-HT biosynthesis and enhances GI motility in  
87 mice (Ge et al., 2018). However, the identity of bacterial species contributing to the  
88 regulation of peripheral serotonin production, the mechanism of action of their serotonin-  
89 stimulating metabolites and their pathophysiological roles in IBS-D remain to be elucidated.  
90 To inform intervention strategies for the treatment of IBS-D, it is imperative to characterize  
91 gut bacteria and identify gut-microbial metabolites that regulate peripheral 5-HT levels in  
92 IBS-D patients.

## 93 **Results**

### 94 **The positive association between *Ruminococcus gnavus*, peripheral serotonin and** 95 **severity of diarrhea symptoms in IBS-D**

96 To understand the role of gut microbiota responsible for the deregulation of peripheral 5-HT  
97 in the pathophysiology of IBS-D, a total of 290 IBS-D patients and 89 healthy controls (HC)  
98 were recruited in our previous study (Zhao et al., 2019) and their biospecimens including  
99 feces, serum and urine were used for analyses. We firstly analysed the serum 5-HT and urine  
100 5-HIAA (a urinary biomarker of 5-HT) levels in this cohort. Consistent with our previous and  
101 other studies (Thijssen et al., 2016; Wong et al., 2019), increased level of peripheral serotonin  
102 (5-HT) was found in the sera from IBS-D patients (Figure.1A). In line with elevated serum 5-  
103 HT level, increased level of urine 5-HIAA was observed in IBS-D patients (Figure.1B). To  
104 identify the gut bacteria that were potentially responsible for the dysregulation of peripheral  
105 5-HT, we performed correlation analysis between gut microbiota and serum 5-HT level in  
106 IBS-D patients. Notably, we found a series of bacteria species positively correlated with  
107 serum 5-HT level in IBS-D patients (Figure.1C and Supplement Table.S1). Among these  
108 bacteria species, *Ruminococcus gnavus*, a culturable gut bacterium with relatively higher  
109 abundance in human gut microbiota, was significantly increased in IBS-D patients  
110 (Figure.1D) and positively correlated with serum 5-HT level in IBS-D patients (Figure.1E).  
111 Furthermore, *R. gnavus* abundances were positively correlated with severity of IBS-D  
112 symptoms assessed by Bristol stool scale in IBS-D patients (Figure.1F). These data  
113 collectively showed that significant changes of bacteria species, particularly *R. gnavus*, may  
114 be associated with altered 5-HT metabolism in IBS-D.

115 **Monoassociation with *Ruminococcus gnavus* stimulated serotonin production, induced**  
116 **diarrhea-like symptoms in accompanied with phenethylamine production**

117 To investigate the pathological role of *R. gnavus* in dysregulated 5-HT production in IBS-D,  
118 we monoassociated pseudo-germ-free mice with a commercially available gut bacteria strain  
119 *Ruminococcus gnavus* (ATCC 29149). Pseudo germ-free mice monoassociated with *R.*  
120 *gnavus* exhibited significantly elevated levels of serum and intestine 5-HT (Figure.2A-B). In  
121 line with the increased 5-HT level in serum and intestine, shortened GI transit time and  
122 increased fecal water content were observed in pseudo germ-free mice monoassociated with  
123 *R. gnavus* (Figure.2C-D). These results demonstrated that monoassociation with *R. gnavus*  
124 led to increased 5-HT production and IBS-D-like symptoms in mice.

125 To further investigate the molecular mechanisms underlying the microbial regulation of 5-HT  
126 production, we performed untargeted metabolomics to identify the changes of fecal  
127 metabolome in pseudo germ-free mice with/without monoassociation with *R. gnavus*. Score  
128 and volcano plots showed dramatic differences in metabolic profiles of fecal samples  
129 between the two groups (Figure.2E and Figure.2F). Notably, a significant elevation of  
130 aromatic trace amines including PEA and TpA was detected in fecal samples of mice  
131 monocolonized with *R. gnavus* (Figure.2F-G). Moreover, the abilities of *R. gnavus* in  
132 converting Phe and Trp into PEA and TpA respectively were validated *in vitro* (Supplement  
133 Figure.S1A-B). These data showed PEA and TpA may be associated with the stimulatory  
134 effects of *R. gnavus* on 5-HT production and GI transit.

135 **The positive association between phenethylamine and peripheral serotonin in IBS-D**

136 To investigate the clinical relevance of our findings obtained from mouse studies, we  
137 examined PEA and TpA levels in our IBS-D patient cohort. Consistently, we found that PEA  
138 was significantly increased in the faeces of IBS-D patients (Figure.3A). In contrast, there was  
139 no significant change in phenylalanine (Phe), the precursor of PEA, in the faeces of IBS-D  
140 patients (Figure.3B). Notably, correlation analysis revealed that fecal PEA level was  
141 positively correlated with *R. gnavus* at a highest r value and p value among other gut bacterial  
142 species in IBS-D patients (Figure.3C and Supplement Table.S2). Furthermore, PEA level was  
143 also positively correlated with the severity of diarrheal symptoms measured by Bristol stool  
144 scale and serum 5-HT level in IBS-D patients (Figure.3D-F). In line with the elevated level of  
145 PEA in IBS-D patients, faecal TpA level, but not Trp level, was also found significantly

146 increased in IBS-D patients ([Supplement Figure.S2A-B](#)) and positively correlated with  
147 Bristol stool scale and serum 5-HT level in IBS-D patients ([Supplement Figure.S2C-D](#)). We  
148 then compared the catalytic ability of gut microbiota from HC and IBS-D in transforming  
149 Phe into PEA as well as Trp into TpA by batch culture using faecal samples *in vitro*. Higher  
150 concentrations of PEA and TpA were detected in the culture medium supplemented with the  
151 bacterial suspension of IBS-D fecal samples ([Figure.3G](#) and [Supplement Figure.S2E](#)),  
152 indicative of high catalytic ability of gut microbiota in processing Phe and Trp into PEA and  
153 TpA in IBS-D patients. These data collectively showed that the changes of fecal PEA and  
154 TpA are positively associated with peripheral 5-HT and severity of diarrheal symptoms in  
155 IBS-D.

### 156 **Phenethylamine accelerates gastrointestinal motility by stimulating serotonin** 157 **biosynthesis**

158 Since fecal PEA level and TpA level was significantly increased in IBS-D patients and  
159 positively correlated with peripheral 5-HT along with diarrhea-related symptoms in IBS-D  
160 patients, we postulated that PEA and TpA stimulate 5-HT production and hence regulate the  
161 GI transit and colonic secretion. To address this hypothesis, we examined the effects of PEA  
162 and TpA on 5-HT production in mouse intestinal tissues *ex vivo* and intestinal organoids *in*  
163 *vitro*. Notably, PEA treatment within the range of pathophysiological concentrations detected  
164 in IBS-D patients significantly enhanced the 5-HT production in a dose-dependent manner in  
165 both mouse intestinal tissues and intestinal organoids ([Figure.4A-B](#)). Similar observations on  
166 the stimulatory effect of PEA on 5-HT production were found in QGP-1 cells, a well-  
167 established human pancreatic endocrine cell line used for studying 5-HT production  
168 ([Supplement Figure.S3A-C](#)). In contrast, treatment with phenylalanine (Phe), the PEA  
169 precursor, and phenylacetic acid (PA), the downstream metabolite of PEA, did not change the  
170 5-HT level in QGP-1 cells ([Supplement Figure.S3D](#)). We then investigated whether PEA  
171 regulates GI transit and colonic secretion in mice by modulating 5-HT production. Notably,  
172 treatment with PEA within the pathophysiological concentrations by oral administration  
173 resulted in significantly enhanced GI transit and fecal water content along with elevated  
174 levels of serum and intestinal 5-HT in mice ([Figure.4C-F](#)). Blockade of 5-HT production by  
175 TPH1 inhibitor LX-1031 did not only effectively inhibited PEA-induced increase in 5-HT  
176 levels ([Figure.4G-H](#)), but also completely suppressed the increased GI transit and fecal water  
177 content in PEA-treated mice ([Figure.4I-J](#)). Similarly, we found that TpA exerted stimulatory



178 effects on intestinal 5-HT production *ex vivo*, *in vivo* and *in vitro* ([Supplement Figure.S3E-G](#)).  
179 In contrast, 5-HT production was not altered by the treatment with precursor (Trp) or  
180 metabolite (IAA) of TpA ([Supplement Figure.S3H](#)). Interestingly, we noticed TpA and PEA  
181 exhibit additive effects on 5-HT production in intestine tissues cultured *ex vivo* ([Supplement](#)  
182 [Figure.S3 I](#)). Collectively, these results demonstrated that PEA and TpA stimulate GI transit  
183 and secretion in a 5-HT-dependent manner.

#### 184 **Phenethylamine stimulates serotonin production via a TAAR1 dependent mechanism**

185 The peripheral 5-HT is synthesized from Trp by TPH1 (Trp to 5-HTP) and AADC (5-HTP to  
186 5-HT) and subsequently metabolized into 5-HIAA by MAO/ALDH (Matthes and Bader,  
187 2018). To further investigate the mechanism underlying the stimulatory effects of PEA on 5-  
188 HT production, we analysed the relative ratios of 5-HTP/Trp, 5-HT/5-HTP and 5-HIAA/5-  
189 HT by determining Trp, 5-HTP and 5-HIAA levels in serum of PEA-treated mice  
190 ([Supplement Figure.S4A-C](#)). In addition to the upregulation of 5-HT, we found that PEA  
191 treatment in a dose-dependent manner also led to the increase in 5-HTP level in the serum of  
192 mice. As a result, 5-HTP/Trp and 5-HT/5-HTP ratios, but not 5-HIAA/5-HT ratio, were  
193 increased in serum of PEA-treated mice ([Figure.5A](#)), suggesting the stimulatory effect of  
194 PEA on 5-HT signaling is likely mediated by biosynthetic pathway (TPH1 and AADC) but  
195 independent of catabolic pathway (MAO/ALDH).

196 Trace amine-associated receptor 1 (TAAR1), a G protein-coupled receptor (GPCR), is a well-  
197 known receptor for PEA (Xie and Miller, 2008). Previous studies revealed that enzymes  
198 responsible for biosynthesis of 5-HT, including TPH1 and AADC, are activated by  
199 downstream mediators of GPCR signaling, namely cyclic AMP-dependent protein kinase A  
200 (PKA) and calcium/calmodulin-dependent kinase (CaMKII) (Duchemin et al., 2000; Kuhn et  
201 al., 1997; Kumer et al., 1997; Neff et al., 2002; Young et al., 1993). We found that PEA  
202 indeed activated PKA and CaMKII, as indicated by the increased phosphorylation of these  
203 proteins in colonic tissues of mice treated with PEA ([Figure.5B-C](#)). PEA-induced activation  
204 of PKA and CaMKII was abolished by inhibition of TAAR1 with specific antagonist EPPTB  
205 ([Figure.5D-E](#)). Consistently, blockade of TAAR1 activities by EPPTB also suppressed PEA-  
206 induced 5-HT production, GI transit and colonic secretion in mice ([Figure.5F-J](#)) as well as 5-  
207 HT elevation in intestine tissues cultured *ex vivo*. In line with these findings, the PEA-  
208 induced reduction in the ratios of 5-HTP/Trp and 5-HT/5-HTP in serum was also abrogated  
209 by EPPTB treatment ([Figure.5I and Supplement Figure.S4D-G](#)). These results suggest that

210 PEA acting through TAAR1 promotes GI transit and increases colonic secretion by  
211 stimulating 5-HT production.

212 **Phenethylamine produced by IBS-D associated gut microbiota enhances serotonin**  
213 **synthesis and gastrointestinal transit *in vivo***

214 To study *in vivo* action of PEA on 5-HT production and GI motility, we integrated the  
215 plasmid expressing tryptophan decarboxylase sequence (TDC), an enzyme that catalyses the  
216 conversion of Phe into PEA and Trp into TpA from *R. gnavus* (strain ATCC 29149), into a  
217 gut microbe *E.coli* K12. Pseudo germ-free mice were colonized with either vector-control *E.*  
218 *coli* or *E. coli* TDC<sup>+</sup> by oral gavage. The successful integration of the plasmid was validated  
219 by PCR analyses and on *in vitro* production of PEA and TpA in LB medium assessed by LC-  
220 MS analyses ([Supplement Figure.S5A-C](#)). Pseudo germ-free mice colonized with *E. coli*  
221 TDC<sup>+</sup> exhibited significantly elevated levels of PEA and TpA in faeces, confirming that *E.*  
222 *coli* TDC<sup>+</sup> strain produced PEA *in vivo* ([Figure.6A](#)). Consistently, increased serum 5-HT  
223 level and fecal water content coupled with shortened GI transit time were observed in mice  
224 colonized with *E. coli* TDC<sup>+</sup> compared with mice with vector-control *E. coli* ([Figure.6B-D](#)  
225 [and Supplement Figure.S5D-E](#)). These results demonstrated engineered bacteria with TDC  
226 produce PEA and TpA *in vivo* to stimulate 5-HT production, leading to accelerated GI transit  
227 and increased colonic secretion. To further investigate whether PEA and TpA-mediated  
228 TAAR1 signaling is involved in the elevation of 5-HT production and diarrhea-like  
229 symptoms induced by *R. gnavus*, we used TAAR1 antagonist EPPTB to block the action of  
230 PEA and TpA on 5-HT production. We showed that *R. gnavus*-induced 5-HT elevation in  
231 serum and intestine, as well as diarrhea-like symptoms including accelerated GI transit and  
232 increased fecal water content, were significantly suppressed by EPPTB treatment ([Figure.6E-](#)  
233 [H and Supplement Figure.S5F-G](#)). These results demonstrated aromatic trace amines-  
234 producing gut bacteria *R. gnavus* modulates 5-HT production and hence GI transits via  
235 PEA/TpA-mediated TAAR1 signalling, suggesting PEA-producing gut bacteria plays an  
236 important role in the pathogenesis of diarrhea symptoms of IBS-D patients.

237 To investigate the therapeutic potential of targeting TAAR1 in the management of IBS-D, we  
238 made use of the mice colonized with gut microbiota derived from IBS-D patients or healthy  
239 control as a preclinical model of IBS-D and treat them with TAAR1 antagonist EPPTB.  
240 Pseudo germ-free mice colonized with IBS-D microbiota exhibited diarrhea-like symptoms  
241 characterized by increased GI transit and defecation frequency, coupled with elevated 5HT

242 biosynthesis and increased production of PEA and TpA in gut. All of these pathological  
243 changes induced by transplantation of IBS-D faecal microbiota were significantly suppressed  
244 by inhibition of TAAR1 activity with EPPTB. These data highlights the therapeutic potential  
245 of targeting PEA/TAAR1 pathway in the management of IBS-D.

## 246 **Discussion**

247 In the present study, we provided mechanistic insights into the contribution of gut microbiota  
248 and its metabolites derived from dietary nutrients to the development of IBS-D by regulating  
249 5-HT production. We herein showed human gut bacterium *R. gnavus* enriched in IBS-D  
250 patients is positively associated with peripheral 5-HT and severity of diarrheal symptoms.  
251 Monoassociation with *R. gnavus* in pseudo germ-free mice stimulated peripheral 5-HT  
252 production and hence induced IBS-D-like symptoms including accelerated GI transit and  
253 increased colonic secretion. Furthermore, we showed PEA and TpA produced by *R. gnavus*-  
254 mediated catabolism of dietary essential amino acids, are responsible for induction of  
255 diarrhea-like symptoms via the stimulation of 5-HT production. To the best of our knowledge,  
256 we are the first to show that PEA and TpA are the direct stimulators of 5-HT biosynthesis,  
257 thereby regulating GI transit and colonic secretion *in vivo* and *ex vivo*. Mechanistically, PEA  
258 and TpA bind to and activate their G-protein coupled receptor (TAAR1) which in turn  
259 mediates 5-HT biosynthesis by stimulating TPH1/AADC activities. To further validate our  
260 observations obtained from *in vitro* studies, we showed that manipulation of endogenous  
261 aromatic trace amines level by colonization of engineered bacteria with TDC led to IBS-D-  
262 like diarrheal symptoms coupled with enhanced 5-HT production. Collectively, these  
263 findings suggest PEA and TpA producers (eg. *R. gnavus*) stimulate 5-HT biosynthesis to  
264 accelerate GI transit via a TAAR1-dependent mechanism, thereafter contributing to diarrheal  
265 symptoms of IBS-D patients. This study demonstrates the causality between gut dysbiosis  
266 and 5-HT-associated diarrheal symptoms and confirms the dysregulation of host-microbe  
267 interaction as one of the leading causes of IBS-D.

268 Although gut microbiota has been shown to modulate peripheral 5-HT and GI motility by  
269 interacting with host EC cells (Agus et al., 2018), the mechanism by which gut-microbial  
270 metabolites affect 5-HT production and their roles in the development of IBS remain largely  
271 unclear. Gut microbial metabolites including butyrate, propionate, tyramine, deoxycholate  
272 and p-aminobenzoate have been shown to stimulate 5-HT biosynthesis *in vitro*, which  
273 provide fundamental understanding to the regulatory mechanisms of gut microbiota in  
274 regulating 5-HT (Yano et al., 2015). However, these metabolites including short fatty acids  
275 (butyrate and propionate) and deoxycholate are not altered in IBS-D patients (Luo et al., 2021;  
276 Wei et al., 2020). Although tyramine was found increased in inflammatory bowel disease  
277 (Santorù et al., 2017) and colorectal cancer (Salahshouri et al., 2021), we could not detect

278 significant changes of tyramine and tyrosine in stool samples and fecal batch culture from  
279 IBS-D patients ([Supplement Figure.S2 F-H](#)). These data suggest that these metabolites may  
280 not contribute to the pathogenesis of IBS-D.

281 In this study, we further confirmed the causal relationship between gut microbiota dysbiosis  
282 and 5-HT dysregulation and their contribution to the pathogenesis of IBS-D. We for the first  
283 time identified human gut bacteria *R. gnavus* as a strong modulator of peripheral 5-HT level.  
284 Metabolically, PEA and TpA produced by *R. gnavus* exert potent stimulatory effects on 5-HT  
285 biosynthesis in intestinal EC cells. PEA, TpA and tyramine are aromatic trace amines  
286 generated from microbial metabolism of dietary aromatic amino acids in the host gut (Liu et  
287 al., 2020). In contrast, their precursors and downstream metabolites do not affect 5-HT  
288 production *in vitro* ([Supplement Figure.S3D/H](#)), suggesting that the regulation of 5-HT  
289 production by microbial breakdown of dietary aromatic amino acids is specifically mediated  
290 by aromatic trace amines. Previous studies showed that TpA drives fluid secretion and alters  
291 GI transit (Bhattarai et al., 2018), and tyramine exhibits direct stimulatory effects on intestine  
292 contraction (Marcobal et al., 2012). Therefore, aromatic trace amines control the GI motility  
293 by simultaneously regulating 5-HT production and its action, potentially explaining why the  
294 efficacy of current pharmacological approaches for treating IBS-D by targeting serotonin  
295 receptor is not satisfactory owing to the continuous activation of 5-HT biosynthesis by  
296 aromatic trace amines with the supply from dietary amino acids.

297 The elevation of TpA and its precursor Trp was detected in stool samples of IBS-D patients  
298 (Mars et al., 2020), and its action on GI motility via activating epithelial 5-HTR4 has been  
299 reported (Bhattarai et al., 2018). In contrast, the 5-HTR4 antagonist, which has been shown to  
300 block the TpA stimulatory action on GI transit (Bhattarai et al., 2018), failed to block the  
301 inducing effects of TpA and PEA on 5-HT production ([Supplement Figure.S4 H](#)). Therefore,  
302 developing new strategies to reduce microbial transformation of dietary amino acids into  
303 aromatic trace amines may pave the way towards precise treatment and eventually the cure of  
304 IBS-D. Gut microbial-produced aromatic trace amines including PEA, TpA and tyramine are  
305 ligands of TAAR1, a G-protein coupled receptor expressed in both central nervous system  
306 and gut (Sotnikova et al., 2009). Dysregulated TAAR1 signaling has been found to be  
307 involved in psychiatric disorders (Dodd et al., 2021) and mood disorders (Alnefeesi et al.,  
308 2021). TAAR1 modulators (agonists) are being studied as novel drugs for schizophrenia,  
309 Parkinson's related psychoses and substance abuse (Dodd et al., 2021). Interestingly, about

310 60% of patients with neuropsychiatric disorders present GI symptoms, such as IBS (Fadgyas-  
311 Stanculete et al., 2014). Deregulation of TAAR1 ligands may therefore be a common factor  
312 in both GI disorders and comorbid neuropsychiatric disorders which can be addressed in  
313 future studies. The present study identified *R. gnavus* as an aromatic trace amines-producer  
314 that stimulates 5-HT production and induces IBS-D-like symptoms in mice. In other studies,  
315 *R. gnavus* has been reported to be associated with inflammatory bowel disease (IBD) (Hall et  
316 al., 2017) and exhibits proinflammatory properties by producing inflammatory  
317 polysaccharides (Henke et al., 2019). In line with these observations, low-grade chronic  
318 inflammation has been found in the colonic tissues of IBS-D patients (Öhman and Simrén,  
319 2010; Rana et al., 2013). These observations suggest that *R. gnavus* may promote  
320 inflammatory responses and impair barrier functions to induce other IBS-D symptoms, such  
321 as abdominal pain and bloating, in addition to increased GI transit and secretion. In fact,  
322 studies has demonstrated that IBS patients indeed are at a greater risk of developing IBD  
323 (Porter et al., 2012). Our findings reveal that mice monoassociated with *R. gnavus* exhibited  
324 increased GI transit and colonic secretion without the presence of fecal occult blood, a major  
325 symptom of IBD, suggesting that *R. gnavus* predominantly contributes to the development of  
326 IBS-D rather than IBD in normal mice but may promote colonic injury in the experimental  
327 model of colitis.

328 Collectively, our findings not only provide new insights into the pathogenesis of IBS-D, but  
329 also lay a foundation for developing therapeutics for the management of 5-HT abnormalities  
330 in IBS-D. There are several limitations in this study. Due to lack of genetic tools to target the  
331 TDC gene in *R. gnavus*, we used TAAR1 antagonist to determine the effects of *R. gnavus*  
332 ATCC 29149 on GI motility and 5-HT production. Our investigation demonstrated that  
333 TAAR1 antagonist effectively abolishes the stimulatory effect of PEA on serotonin  
334 biosynthesis *in vitro* and *in vivo*, suggesting that the *in vivo* action of PEA is primarily  
335 mediated via TAAR1 in the context of gut motility. These studies highlight the therapeutic  
336 potential of targeting TAAR1 or microbial TDC enzyme in the treatment of IBS-D. However,  
337 other receptors, such as 5-HT4R, may also mediate the actions of aromatic trace amines such  
338 as TpA (Bhattarai et al., 2018), which should be addressed in the future studies.

### 339 **Acknowledgements**

340 This work was kindly funded by the National Natural Science Foundation of China  
341 (82000504, 81973538), General Research Fund (12102620 and 12102721) and Innovation

342 and Technology Fund (ITS/148/14FP). We are thankful to all patients and healthy volunteers  
343 who donated specimens for this study.

#### 344 **Author contributions**

345 ZX.B. and XHL.W conceptualized the project and designed the experiments. ZW.N. and  
346 LX.Z. conducted metabolites quantification in serum, urine and fecal samples of IBS-D  
347 patients. LX.Z., CH.H., YJ.Z. and M.Z. performed *in vivo* and *in vitro* study. W.Y  
348 contributed to the management and recourses of clinical specimens. XL.W contributed to  
349 bacterial culture and engineering. JJ.W. and EL.Z. contributed to metagenomic data analysis.  
350 LX.Z. and XHL.W analyzed data and wrote the manuscript with the input of co-authors.  
351 HT.X., L.Z., YY.L., CFW.C., JD.H., SF.Y. and KM.C. contribute to the study design,  
352 technical support and data analysis support towards this work.

#### 353 **Declaration of interests**

354 The authors have claimed no financial interests to declare.

## 355 **Figure legends**

356 Figure.1 *R. gnavus* significantly increased in IBS-D patients and positively correlated with  
357 serum 5-HT level and diarrhea symptoms. (A-B) Serum 5-HT and urine 5-HIAA level in HC  
358 (n=89) and IBS-D (n=290) subjects. (C) Spearman r value and p value of gut bacteria species  
359 abundances and serum 5-HT level in IBS-D patients. (D) Relative abundances of selected gut  
360 bacteria species in HC and IBS-D subjects. (E) Spearman's correlation between relative  
361 abundances of *R. gnavus* with serum 5-HT level in IBS-D subjects. (F) Spearman's  
362 correlation between relative abundances of *R. gnavus* with Bristol Stool Scale in IBS-D  
363 subjects. Differences of relative abundances of *R. gnavus* in HC and IBS-D patients were  
364 analyzed by one-tailed Mann-Whitney test. Data are presented as mean  $\pm$  S.E.M.

365 Figure.2 *R. gnavus* induces elevated 5-HT production and diarrhea-like symptoms in  
366 accompanied with PEA and TpA production in mice. (A) Serum and intestine 5-HT level in  
367 pseudo germ-free mice after monoassociation with/without *R. gnavus* (ATCC 29149)  
368 (n=6/group). (C-D) GI transit time and fecal water content indexes in pseudo germ-free mice  
369 after monoassociation with/without *R. gnavus* (ATCC 29149) (n=6/group). (E) Score plot of  
370 fecal metabolome in pseudo germ-free mice after monoassociation with/without *R. gnavus*  
371 (ATCC 29149) (n=6/group). (F) Volcano plot of fecal metabolome in pseudo germ-free mice  
372 after monoassociation with/without *R. gnavus* (ATCC 29149) (n=6/group). (G) Fecal PEA  
373 and TpA level in pseudo germ-free mice after monoassociation with/without *R. gnavus*  
374 (ATCC 29149) (n=6/group). Differences of serum and intestine 5-HT level and GI transit  
375 time and fecal water content indexes in mice were analyzed by two-tailed student t-test.  
376 Differences of fecal PEA and TpA level in mice were analyzed by one-tailed student t-test.  
377 Data are presented as mean  $\pm$  S.D. [See also Supplement Figure.S1.](#)

378 Figure.3 Fecal PEA and TpA are increased and positively correlated with serum 5-HT level  
379 in IBS-D patients. (A-B) PEA and Phe level in fecal samples of in HC (n=89) and IBS-D  
380 (n=290) subjects. (C) Spearman r value and p value of gut bacteria species abundances and  
381 fecal PEA level in IBS-D patients. (D-F) Spearman's correlation between fecal PEA level  
382 with *R. gnavus* abundances, Bristol Stool Scale and serum 5-HT level in IBS-D subjects. (G)  
383 PEA level in batch culture samples using feces from HC and IBS-D (n=30/group).  
384 Differences of fecal PEA and Phe level in HC and IBS subjects as well as batch culture  
385 samples were analyzed by one-tailed Mann-Whitney test. Data are presented as mean  $\pm$   
386 S.E.M. [See also Supplement Figure.S2.](#)



387 Figure.4 PEA and TpA activates 5-HT production, accelerates GI transit and increase colonic  
388 secretion *in vitro* and *in vivo*. (A) 5-HT level in mice *ex vivo* intestinal tissues after treatment  
389 of PEA as indicated concentration (25 $\mu$ M, 50 $\mu$ M and 100 $\mu$ M) or control for 2 hours  
390 (n=3/group). (B) 5-HT level in mice *in vitro* intestinal organoids after treatment of PEA as  
391 indicated concentration (25 $\mu$ M and 50 $\mu$ M) or control for 4 hours (n=3/group). (C-D) 5-HT  
392 level in mice serum and intestinal tissues after treatment of PEA as indicated dosages  
393 (2mg/kg, 5mg/kg and 10mg/kg) or control (water) (n=6/group). (E-F) Fecal water content  
394 and GI transit time in mice after treatment of PEA as indicated dosages (2mg/kg, 5mg/kg and  
395 10mg/kg) or control (water) (n=6/group). (G-H) 5-HT level in mice serum and intestinal  
396 tissues after treatment of PEA (10mg/kg), TPH1 inhibitor (LX-1031, 50mg/kg) or control  
397 (water) (n=6/group). (I-J) Fecal water content and GI transit time in mice after treatment of  
398 PEA (10mg/kg) and TPH1 inhibitor (LX-1031, 50mg/kg) or control (water) (n=6/group).  
399 Differences of 5-HT level, GI transit time and fecal water content were analyzed by t-test  
400 (two-tailed Mann-Whitney test) or ordinary one-way ANOVA. Data are presented as mean  $\pm$   
401 S.D. [See also Supplement Figure.S3.](#)

402 Figure.5 PEA stimulates 5-HT production via a TAAR1 dependent mechanism. (A) 5-HT  
403 biosynthesis and metabolism profiles after treatment of PEA as indicated dosages (2mg/kg,  
404 5mg/kg and 10mg/kg) or control (water) (n=6/group). (B-C) Western blot (and semi-  
405 quantification) in proximal colonic tissues of mice after treatment of PEA as indicated  
406 dosages (2mg/kg, 5mg/kg and 10mg/kg) or control (water) (n=3/group). (D-E) Western blot  
407 (and semi-quantification) in proximal colonic tissues of mice after treatment of PEA  
408 (10mg/kg) and TAAR1 antagonist EPPTB (10mg/kg) or control (1% DMSO in saline)  
409 (n=3/group). (F-G) GI transit time and fecal water content in mice after treatment of PEA  
410 (10mg/kg) and TAAR1 antagonist EPPTB (10mg/kg) or control (1% DMSO in saline)  
411 (n=6/group). (H) 5-HT level in mice serum after treatment of of PEA (10mg/kg) and TAAR1  
412 antagonist EPPTB (10mg/kg) or control (1% DMSO in saline) (n=6/group). (I) 5-HT  
413 biosynthesis and metabolism profiles after treatment of PEA (10mg/kg) and TAAR1  
414 antagonist EPPTB (10mg/kg) or control (1% DMSO in saline) (n=6/group). (J) 5-HT level in  
415 mice *in vitro* intestinal tissues after treatment of PEA (50 $\mu$ M) and TAAR1 antagonist EPPTB  
416 (50 $\mu$ M) or control (1% DMSO) (n=3/group). Differences of 5-HT level, GI transit time and  
417 fecal water content were analyzed using ordinary one-way ANOVA. Data are presented as  
418 mean  $\pm$  S.D. [See also Supplement Figure.S4.](#)

419 Figure.6 *In vivo* PEA and TpA produced by IBS-D associated bacteria enhances 5-HT  
420 synthesis and induce diarrhea-like symptoms. (A) Fecal PEA level in pseudo germ-free mice  
421 after monoassociation with *E.coli* vector control or *E.coli* TDC<sup>+</sup> (n=6/group). (B-D) Serum 5-  
422 HT level, GI transit time and fecal water content in pseudo germ-free mice after  
423 monoassociation with *E.coli* vector control or *E.coli* TDC<sup>+</sup> (n=6/group). (E-H) Fecal PEA  
424 level, serum 5-HT level, GI transit time and fecal water content in pseudo germ-free mice  
425 after monoassociation with *R. gnavus* (ATCC 29149) and TAAR1 antagonist EPPTB  
426 (10mg/kg) or control (1% DMSO in saline) (n=6/group). (I-L) Fecal PEA level, colon 5-HT  
427 level, GI transit time and defecation frequency in pseudo germ-free mice after  
428 monoassociation with gut microbiota from HC (n=8) and IBS-D (n=8) subjects and TAAR1  
429 antagonist EPPTB (10mg/kg) or control (1% DMSO in saline) (n=6/group). Differences of  
430 PEA level, 5-HT level in serum and intestine, GI transit time defecation frequency were  
431 analyzed using student t-test (two-tailed Mann-Whitney test) or ordinary one-way ANOVA.  
432 Data are presented as mean  $\pm$  S.D. [See also Supplement Figure.S5.](#)

433 **STAR Methods**

434 **Reagent and resources sharing contact**

435 Further information and requests for resources and reagents can be directed to and will be  
436 fulfilled by the Lead Contact Zhao-xiang Bian ([bxxiang@hkbu.edu.hk](mailto:bxxiang@hkbu.edu.hk)).

437 **Experimental models and subject details**

438 Human study

439 To determine the changes of phenethylamine and 5-HT signaling in IBS-D patients, the  
440 human study was conducted as previously described (Zhao et al., 2019). Briefly, IBS-D  
441 patients (n=345) and healthy volunteers (n=91) were recruited following the required criteria  
442 in this previous study. Written consent was obtained from each subject before the collection  
443 of their specimens. Biological samples including serum, urine and feces of all subjects were  
444 collected and transported to the laboratory in dry ice and stored in -80 °C. Details of clinical  
445 indexes and diagnostic data of all subjects can be found in Supplementary.

446 Mouse study

447 The mice study was approved by the Committee on the Use of Human & Animal Subjects in  
448 Teaching & Research at Hong Kong Baptist University (Hong Kong SAR, China). All  
449 experiments were performed under the regulation of the Animals (Control of Experiments)  
450 Ordinance of the Department of Health, Hong Kong SAR, China. Male C57BL/6 mice aged  
451 6-8 weeks and weighed 20-25g were purchased from Laboratory Animal Services Centre,  
452 The Chinese University of Hong Kong (Hong Kong SAR, China) and raised in Animal Unit,  
453 School of Chinese Medicine, Hong Kong Baptist University. The mice were housed at a  
454 condition of 12 h light/dark cycle in a controlled temperature of around 25°C with free access  
455 to food and water. The *in vivo* experiments were reported following ARRIVE guidelines (du  
456 Sert et al., 2020).

457 Organoids

458 Intestinal organoids were obtained from small intestines of 8-10 week old C57BL6 mice as  
459 previously described (Wong et al., 2019). Briefly, the mice were euthanized by carbon

460 dioxide and their small intestine were isolated and flushed with ice-cold phosphate-buffered  
461 saline (PBS). The intestinal segments were obtained by longitudinal incision and incubated in  
462 Gentle Cell Dissociation Reagent (STEMCELL Technology) with gentle shaking at room  
463 temperature for 15 min. The intestinal segments were then filtered using a 70- $\mu$ m cell  
464 strainer to get the cells of the intestinal crypts. About 500 crypts were grown in the matrix gel  
465 in supplement with advanced DMEM/F12 medium and growth-factor-reduced Matrigel in a  
466 ratio of 1:3. The standard medium was replaced with advanced DMEM/F12 medium in  
467 supplement with 2 mM Glutamax, 10 mM HEPES, 1mM N-acetyl-cysteine, B27  
468 supplement, N2 supplement, recombinant murine EGF (50 ng/ml), recombinant human R-  
469 spondin 1 (500 ng/ml), and recombinant murine Noggin (50 ng/ml). For experiments  
470 evaluating the effects of phenethylamine on 5-HT level and EC cell differentiation, organoids  
471 were treated with/without phenethylamine at indicated dosages.

#### 472 QGP-1 cells

473 QGP-1 cells were cultured in RPMI 1640 medium supplement with 10% FBS. QGP-1 cells  
474 are a human pancreatic endocrine cell line that can produce 5-HT (Doihara et al., 2009). For  
475 experiments evaluating the effects of phenylalanine, phenethylamine and phenylacetic acid  
476 on 5-HT production, QGP-1 cells were treated with/without phenylalanine, phenethylamine  
477 and phenylacetic acid at indicated dosages and time.

#### 478 Bacteria strains

479 *Ruminococcus gnavus* (strain ATCC 29149) was firstly grown on Tryptic soy broth (TSB)  
480 agar plate and cultured in TSB broth using single colony. *R. gnavus* (strain ATCC 29149)  
481 was collected from the medium by centrifuge at 3, 500 rpm for 10 min at room temperature.  
482 These bacteria strains were then prepared in 200  $\mu$ L sterilized PBS and then delivered to  
483 pseudo germ-free mice by oral gavage. Fecal samples were collected daily for measurement  
484 of fecal phenethylamine levels in pseudo germ-free mice before and after oral administration  
485 of bacteria strains.

486 Phenethylamine-producing *E.coli* K12 was constructed using the tryptophan decarboxylase  
487 (TDC) gene (A7B1V0) from *R. gnavus*. The TDC gene was cloned into the vector and the  
488 resulting plasmid was transferred into *E.coli* K12 as previously described (Kelpšas and  
489 Wachenfeldt, 2019). The insertion of the TDC gene into the *E.coli* K12 was confirmed by

490 PCR and *in vitro* phenethylamine production in LB broth containing 0.25% phenylalanine. A  
491 vector-only control strain of *E.coli* K12 was also constructed. These bacteria strains were also  
492 collected as previously described and prepared in 200  $\mu$ L sterilized PBS and then delivered to  
493 pseudo germ-free mice by oral gavage.

#### 494 **Study methods details**

##### 495 Pseudo germ-free mouse model

496 An broad-spectrum antibiotics mixture (ABX) containing vancomycin (100 mg/kg),  
497 neomycin (200 mg/kg), metronidazole (200 mg/kg) and ampicillin (200 mg/kg) was used to  
498 establish a pseudo-germ-free model in mice. Briefly, the antibiotics mixture was administered  
499 to mice by oral gavage for 10 consecutive days in prior to fecal microbial transplantation  
500 (FMT) or monocolonization study (Kennedy et al., 2018).

##### 501 Metabolites quantification

502 An Agilent 1290 Infinity II UPLC system coupled to a triple quadrupole (QQQ) 6470 mass  
503 spectrometry was used for targeted metabolomics profiling study. A Waters BEH 2.1x50mm  
504 C18 1.7 $\mu$ m column with a pre-column was used. The mobile phase used in LC-MS-QQQ was  
505 A: water with 0.1% formic acid and B: acetonitrile with 0.1% formic acid. The gradients  
506 were set as 2% B (0-0.5 min), 2%-30% B (0.5-4 min), 30%-100% B (4-6 min), 100% B (6-8  
507 min), 100%-2% B (8-8.1 min) and maintain in 2% B (8.1-10 min). The MS data were  
508 collected and processed by in-house software provided by Agilent. The standards list, MRM  
509 transition, fragmentor and collision energy and are listed in ([Supplement Table.S3](#)).  
510 Correlation analysis was conducted among serum 5-HT level, fecal PEA level and diarrhea-  
511 related symptoms in IBS-D patients. The spearman's rank coefficient correlation analysis  
512 was used for correlations and the significant cut-off value was set at an FDR adjusted *p*-value  
513 <0.05.

##### 514 Batch culture of fecal samples

515 About 50 mg fecal samples were mixed with 20x sterilized 1x PBS (m/v) and homogenized  
516 with tissuelyzer after adding steel beads. 20  $\mu$ L fecal suspension from each sample was  
517 inoculated in 2mL TSB supplemented with 0.25% Phe and incubated overnight under  
518 anaerobic conditions at 37°C. After incubation, 100  $\mu$ L medium was then used to determine

519 Phe and PEA levels. Briefly, 400  $\mu$ L MeOH was added to 100  $\mu$ L medium and vigorously  
520 vortexed. After that, the mixture was centrifuged at 15,000 rpm for 10 min at 4 °C. 200  $\mu$ L  
521 supernatant was used for LC-MS analysis.

#### 522 Phenethylamine administration

523 To study phenethylamine effect on 5-HT production, phenethylamine at a dosage of 2mg/kg,  
524 5mg/kg and 10mg/kg (dissolved in 0.5% CMC-Na) were administered to mice by oral gavage.  
525 After 15 min, mice treated with/without phenethylamine were sacrificed under isoflurane  
526 anesthesia and serum samples and fresh proximal colon and distal colon tissues were  
527 collected and stored at -80 °C until analysis.

#### 528 *In vivo* measurements

529 Fecal pellet water content test: 1.5 mL Eppendorf tubes were pre-weighed and were used to  
530 collect fecal pellets from mice immediately after defecation. The tubes were then tightly  
531 closed to measure the wet weight. Afterward, the tubes were opened and placed in an oven at  
532 60 °C overnight to measure the dry weight. Fecal pellet water content was measured by  
533 subtracting dry weight from wet weight and normalizing it to the wet pellet mass. Fecal  
534 pellets from mice are also counted after defecation within 2 hours for defecation frequency  
535 test.

536 Carmine Red Assay: Mice were given 300  $\mu$ L 6% carmine red solution (prepared by 0.5%  
537 methylcellulose) by oral gavage to measure the GI transit time after treatment with  
538 phenethylamine with indicated dosages. The mice were put on white sheet paper to track the  
539 red pellet in their cages after oral gavage. Total taken time for the appearance of the first red  
540 pellet after oral gavage was recorded as gut transit time.

#### 541 Western blotting analysis

542 Colonic tissues were lysed in RIPA buffer with protease inhibitor cocktails in a tissuelyzer.  
543 The tissue lysates were then centrifuged at 15,000 rpm for 15 min at 4 °C and quantified by  
544 BCA kit for their protein concentration. The normalized supernatant was mixed with 5x  
545 loading buffer and heated at 98 °C on a dry bath for 10 min. The samples were then  
546 determined according to the western blotting protocol provided by Abcam. The blots were

547 incubated with HRP-linked anti-rabbit IgG or anti-mouse IgG and reacted with enhanced  
548 chemiluminescence.

549 Transplantation of human microbiota (FMT) in pseudo-germ-free mice

550 Fecal samples of HC and IBS-D subjects (n=8/group) were prepared as suspensions in PBS at  
551 a concentration of (100 mg/mL). ABX-treated pseudo germ-free mice were used as recipient  
552 of HC and IBS-D microbiota and were daily orally gavaged with human microbiota  
553 suspension at a dosage of 500mg/kg for 5 consecutive days. After FMT, GI transit, stool  
554 consistency and defecation frequency were measured. Fecal samples were collected at prior  
555 to FMT (after ABX intervention) and after FMT.

556 Phenethylamine-producing bacteria analysis in IBS-D patients

557 Metagenomics data of IBS-D patients and healthy volunteers were obtained as previously  
558 described (Han et al., 2021). Correlation analysis was conducted between serum 5-HT level  
559 and fecal PEA level with PEA-producing bacteria in IBS-D patients. The spearman's rank  
560 coefficient correlation analysis was used for correlations and the significant cut-off value was  
561 set at an FDR adjusted  $p < 0.05$ .

## 562 **Statistical analysis**

563 Results were from multiple, at least three times independent experiments. Data were  
564 expressed as average and SD or SEM values of at least triplicate samples. Significance  $p$ -  
565 values were calculated using GraphPad Prism 8 and the  $p$ -value less than 0.05 was regarded  
566 as statistically significant. Wilcoxon rank-sum two-tailed test was used to determine  
567 metabolites difference between IBS-D and healthy subjects. Wilcoxon one-tailed test was  
568 used to determine IBS-D-associated gut microbiota produces higher phenethylamine in  
569 metagenomics data. Unpaired student's  $t$ -tests or one-way ANOVA were used in other  
570 experiments as indicated.

571 **Supplemental information**

572 Supplement Figure.S1 *R. gnavus* induces elevated 5-HT production and diarrhea-like  
573 symptoms. (A-B) LC-MS chromatogram of PEA and TpA level in tryptic soy broth culture  
574 medium of *R. gnavus* (ATCC 29149).

575 Supplement Figure.S2 Fecal PEA and TpA are increased in IBS-D patients and positively  
576 correlated with serum 5-HT level. (A-B) Fecal TpA and Trp level in fecal samples of HC and  
577 IBS-D subjects. (C-D) Spearman's correlation between fecal TpA with relative abundances  
578 of *R. gnavus* and Bristol Stool Scale in IBS-D subjects. (E) TpA level in batch culture  
579 samples using feces from HC and IBS-D (n=30/group). (F-G) Fecal tyramine and tyrosine  
580 level in HC and IBS subjects. (H) Tyramine level in batch culture samples using feces from  
581 HC and IBS-D (n=30/group). Differences of fecal TpA, Trp, tyramine and tyrosine level in  
582 HC and IBS subjects as well as batch culture samples were analyzed by one-tailed Mann-  
583 Whitney test. Data are presented as mean  $\pm$  S.E.M.

584 Supplement Figure.S3 PEA and TpA activates 5-HT production, accelerates GI transit and  
585 increase colonic secretion *in vitro* and *in vivo*. (A-B) 5-HT level in QGP-1 cells after  
586 treatment of PEA as indicated concentration (25 $\mu$ M, 50 $\mu$ M and 100 $\mu$ M) or control for 4  
587 hours and 24 hours (n=3/group). (C) IF staining of 5-HT in QGP-1 cells after treatment of  
588 PEA 25 $\mu$ M or control for 24 hours (n=3/group). (D) 5-HT level in QGP-1 cells after  
589 treatment of PAA or Phe as indicated concentration (50 $\mu$ M, 100 $\mu$ M and 200 $\mu$ M) or control  
590 for 24 hours (n=3/group). (E-F) 5-HT level in mice intestinal tissues and serum after  
591 treatment of TpA as indicated dosages (2mg/kg, 5mg/kg and 10mg/kg) or control (water)  
592 (n=6/group). (G) 5-HT level in QGP-1 cells after treatment of TpA as indicated concentration  
593 (25 $\mu$ M, 50 $\mu$ M and 100 $\mu$ M) or control for 24 hours (n=3/group). (H) 5-HT level in QGP-1  
594 cells after treatment of IAA or Trp as indicated concentration (50 $\mu$ M, 100 $\mu$ M and 200 $\mu$ M) or  
595 control for 24 hours (n=3/group). (I) 5-HT level in mice intestinal tissues *ex vivo* after  
596 treatment of TpA and PEA as indicated dosages (50 $\mu$ M) (n=3/group). Differences of 5-HT in  
597 mice serum and intestine tissues and QGP-1 cells were analyzed by ordinary one-way  
598 ANOVA. Data are presented as mean  $\pm$  S.D.

599 Supplement Figure.S4 PEA stimulates 5-HT production via a TAAR1 dependent mechanism.  
600 (A-C) Serum Trp, 5-HTP and 5-HIAA in mice intestinal tissues and serum after treatment of



601 TpA as indicated dosages (2mg/kg, 5mg/kg and 10mg/kg) or control (water) (n=6/group). (D-  
602 G) Serum Trp, 5-HTP, 5-HT and 5-HIAA in mice after treatment of PEA (10mg/kg) and  
603 TAAR1 antagonist EPPTB (10mg/kg) or control (1% DMSO in saline) (n=6/group).  
604 Differences of Trp, 5-HTP, 5-HT and 5-HIAA in mice serum and intestine tissues were  
605 analyzed by ordinary one-way ANOVA. Data are presented as mean  $\pm$  S.D.

606 Supplement Figure.S5 *In vivo* PEA and TpA produced by IBS-D associated bacteria  
607 enhances 5-HT synthesis and induce diarrhea-like symptoms. (A) PCR electrophoresis of  
608 positive clone of *E.coli* with TDC gene. (B-C) LC-MS chromatogram of PEA and TpA level  
609 in LB culture medium of *E.coli* TDC+ and *E.coli* vector control.

610 Supplement Table.S1 Spearman's correlation between serum 5-HT with gut bacteria species  
611 in IBS-D patients.

612 Supplement Table.S2 Spearman's correlation between fecal PEA with gut bacteria species in  
613 IBS-D patients.

614 Supplement Table.S3 MRM transition and parameters used for metabolites quantification.

615 Supplement Table.S4 Fecal PEA level in selected HC and IBS-D subjects for FMT  
616 experiment

617 **References**

- 618 Agus, A., Planchais, J., and Sokol, H. (2018). Gut Microbiota Regulation of Tryptophan  
619 Metabolism in Health and Disease. *Cell Host Microbe* 23, 716–724.
- 620 Alnefeesi, Y., Tamura, J.K., Lui, L.M.W., Jawad, M.Y., Ceban, F., Ling, S., Nasri, F.,  
621 Rosenblat, J.D., and McIntyre, R.S. (2021). Trace amine-associated receptor 1 (TAAR1):  
622 Potential application in mood disorders: A systematic review. *Neurosci. Biobehav. Rev.* 131,  
623 192–210.
- 624 Bellono, N.W., Bayrer, J.R., Leitch, D.B., Castro, J., Zhang, C., O'Donnell, T.A., Brierley,  
625 S.M., Ingraham, H.A., and Julius, D. (2017). Enterochromaffin cells are gut chemosensors  
626 that couple to sensory neural pathways. *Cell* 170, 185–198.
- 627 Bhattarai, Y., Williams, B.B., Battaglioli, E.J., Whitaker, W.R., Till, L., Grover, M., Linden,  
628 D.R., Akiba, Y., Kandimalla, K.K., and Zachos, N.C. (2018). Gut microbiota-produced  
629 tryptamine activates an epithelial G-protein-coupled receptor to increase colonic secretion.  
630 *Cell Host Microbe* 23, 775–785.
- 631 Dodd, S., F. Carvalho, A., Puri, B.K., Maes, M., Bortolasci, C.C., Morris, G., and Berk, M.  
632 (2021). Trace Amine-Associated Receptor 1 (TAAR1): A new drug target for psychiatry?  
633 *Neurosci. Biobehav. Rev.* 120, 537–541.
- 634 Doihara, H., Nozawa, K., Kojima, R., Kawabata-Shoda, E., Yokoyama, T., and Ito, H. (2009).  
635 QGP-1 cells release 5-HT via TRPA1 activation; a model of human enterochromaffin cells.  
636 *Mol. Cell. Biochem.* 331, 239–245.
- 637 Duchemin, A., Berry, M.D., Neff, N.H., and Hadjiconstantinou, M. (2000). Phosphorylation  
638 and activation of brain aromatic L-amino acid decarboxylase by cyclic AMP-dependent  
639 protein kinase. *J. Neurochem.* 75, 725–731.
- 640 Dunlop, S.P., Jenkins, D., Neal, K.R., and Spiller, R.C. (2003). Relative importance of  
641 enterochromaffin cell hyperplasia, anxiety, and depression in postinfectious IBS.  
642 *Gastroenterology* 125, 1651–1659.
- 643 Fadgyas-Stanculete, M., Buga, A.-M., Popa-Wagner, A., and Dumitrascu, D.L. (2014). The  
644 relationship between irritable bowel syndrome and psychiatric disorders: from molecular  
645 changes to clinical manifestations. *J. Mol. Psychiatry* 2, 4.
- 646 Ge, X., Pan, J., Liu, Y., Wang, H., Zhou, W., and Wang, X. (2018). Intestinal crosstalk  
647 between microbiota and serotonin and its impact on gut motility. *Curr. Pharm. Biotechnol.* 19,

- 648 190–195.
- 649 Hall, A.B., Yassour, M., Sauk, J., Garner, A., Jiang, X., Arthur, T., Lagoudas, G.K., Vatanen,  
650 T., Fornelos, N., and Wilson, R. (2017). A novel *Ruminococcus gnavus* clade enriched in  
651 inflammatory bowel disease patients. *Genome Med.* 9, 1–12.
- 652 Han, L., Zhao, L., Zhou, Y., Yang, C., Xiong, T., Lu, L., Deng, Y., Luo, W., Chen, Y., Qiu,  
653 Q., et al. (2021). Altered metabolome and microbiome features provide clues in  
654 understanding irritable bowel syndrome and depression comorbidity. *ISME J.*
- 655 Henke, M.T., Kenny, D.J., Cassilly, C.D., Vlamakis, H., Xavier, R.J., and Clardy, J. (2019).  
656 &lt;em><i>Ruminococcus gnavus</i></em>, a member of the human gut microbiome  
657 associated with Crohn’s disease, produces an inflammatory polysaccharide. *Proc. Natl. Acad.*  
658 *Sci.* 116, 12672 LP – 12677.
- 659 Van den Houte, K., Colomier, E., Schol, J., Carbone, F., and Tack, J. (2020). Recent  
660 advances in diagnosis and management of irritable bowel syndrome. *Curr. Opin. Psychiatry*  
661 33, 460–466.
- 662 Jeffery, I.B., Das, A., O’Herlihy, E., Coughlan, S., Cisek, K., Moore, M., Bradley, F., Carty,  
663 T., Pradhan, M., Dwibedi, C., et al. (2020). Differences in Fecal Microbiomes and  
664 Metabolomes of People With vs Without Irritable Bowel Syndrome and Bile Acid  
665 Malabsorption. *Gastroenterology* 158, 1016-1028.e8.
- 666 Kelpšas, V., and Wachenfeldt, C. von (2019). Strain improvement of *Escherichia coli* K-12  
667 for recombinant production of deuterated proteins. *Sci. Rep.* 9, 17694.
- 668 Kendig, D.M., and Grider, J.R. (2015). Serotonin and colonic motility. *Neurogastroenterol.*  
669 *Motil.* 27, 899–905.
- 670 Kennedy, E.A., King, K.Y., and Baldrige, M.T. (2018). Mouse microbiota models:  
671 comparing germ-free mice and antibiotics treatment as tools for modifying gut bacteria. *Front.*  
672 *Physiol.* 1534.
- 673 Kuhn, D.M., Arthur Jr, R., and States, J.C. (1997). Phosphorylation and activation of brain  
674 tryptophan hydroxylase: identification of serine 58 as a substrate site for protein kinase A. *J.*  
675 *Neurochem.* 68, 2220–2223.
- 676 Kumer, S.C., Mockus, S.M., Rucker, P.J., and Vrana, K.E. (1997). Amino-terminal analysis  
677 of tryptophan hydroxylase: protein kinase phosphorylation occurs at serine 58. *J.*  
678 *Neurochem.* 69, 1738–1745.

- 679 Liu, Y., Hou, Y., Wang, G., Zheng, X., and Hao, H. (2020). Gut Microbial Metabolites of  
680 Aromatic Amino Acids as Signals in Host–Microbe Interplay. *Trends Endocrinol. Metab.*
- 681 Luo, M., Zhuang, X., Tian, Z., and Xiong, L. (2021). Alterations in short-chain fatty acids  
682 and serotonin in irritable bowel syndrome: a systematic review and meta-analysis. *BMC*  
683 *Gastroenterol.* *21*, 14.
- 684 Marcobal, A., De Las Rivas, B., Landete, J.M., Tabera, L., and Muñoz, R. (2012). Tyramine  
685 and phenylethylamine biosynthesis by food bacteria. *Crit. Rev. Food Sci. Nutr.* *52*, 448–467.
- 686 Mars, R.A.T., Yang, Y., Ward, T., Houtti, M., Priya, S., Lekatz, H.R., Tang, X., Sun, Z.,  
687 Kalari, K.R., and Korem, T. (2020). Longitudinal multi-omics reveals subset-specific  
688 mechanisms underlying irritable bowel syndrome. *Cell* *182*, 1460–1473.
- 689 Matthes, S., and Bader, M. (2018). Peripheral serotonin synthesis as a new drug target.  
690 *Trends Pharmacol. Sci.* *39*, 560–572.
- 691 Neff, N.H., Duchemin, A., and Hadjiconstantinou, M. (2002). Activation of aromatic  
692 L-amino acid decarboxylase by calcium/calmodulin kinase II. *J. Neurochem.* *81*, 98–99.
- 693 Öhman, L., and Simrén, M. (2010). Pathogenesis of IBS: role of inflammation, immunity and  
694 neuroimmune interactions. *Nat. Rev. Gastroenterol. Hepatol.* *7*, 163–173.
- 695 De Palma, G., Lynch, M.D.J., Lu, J., Dang, V.T., Deng, Y., Jury, J., Umeh, G., Miranda,  
696 P.M., Pastor, M.P., and Sidani, S. (2017). Transplantation of fecal microbiota from patients  
697 with irritable bowel syndrome alters gut function and behavior in recipient mice. *Sci. Transl.*  
698 *Med.* *9*.
- 699 Porter, C.K., Cash, B.D., Pimentel, M., Akinseye, A., and Riddle, M.S. (2012). Risk of  
700 inflammatory bowel disease following a diagnosis of irritable bowel syndrome. *BMC*  
701 *Gastroenterol.* *12*, 55.
- 702 Rana, S. V, Sharma, S., Sinha, S.K., Parsad, K.K., Malik, A., and Singh, K. (2013). Pro-  
703 inflammatory and anti-inflammatory cytokine response in diarrhoea-predominant irritable  
704 bowel syndrome patients. *Trop. Gastroenterol.* *33*, 251–256.
- 705 Reigstad, C.S., Salmonson, C.E., III, J.F.R., Szurszewski, J.H., Linden, D.R., Sonnenburg,  
706 J.L., Farrugia, G., and Kashyap, P.C. (2015). Gut microbes promote colonic serotonin  
707 production through an effect of short-chain fatty acids on enterochromaffin cells. *FASEB J.*  
708 *29*, 1395–1403.
- 709 Salahshouri, P., Emadi-Baygi, M., Jalili, M., Khan, F.M., Wolkenhauer, O., and Salehzadeh-

- 710 Yazdi, A. (2021). A metabolic model of intestinal secretions: the link between human  
711 microbiota and colorectal cancer progression. *Metabolites* *11*, 456.
- 712 Santoru, M.L., Piras, C., Murgia, A., Palmas, V., Camboni, T., Liggi, S., Ibba, I., Lai, M.A.,  
713 Orrù, S., Blois, S., et al. (2017). Cross sectional evaluation of the gut-microbiome  
714 metabolome axis in an Italian cohort of IBD patients. *Sci. Rep.* *7*, 9523.
- 715 du Sert, N.P., Hurst, V., Ahluwalia, A., Alam, S., Avey, M.T., Baker, M., Browne, W.J.,  
716 Clark, A., Cuthill, I.C., and Dirnagl, U. (2020). The ARRIVE guidelines 2.0: updated  
717 guidelines for reporting animal research. *BMJ Open Sci.* *4*, e100115.
- 718 Sotnikova, T.D., Caron, M.G., and Gainetdinov, R.R. (2009). Trace amine-associated  
719 receptors as emerging therapeutic targets. *Mol. Pharmacol.* *76*, 229–235.
- 720 Sperber, A.D., Dumitrascu, D., Fukudo, S., Gerson, C., Ghoshal, U.C., Gwee, K.A., Hungin,  
721 A.P.S., Kang, J.-Y., Minhu, C., and Schmulson, M. (2017). The global prevalence of IBS in  
722 adults remains elusive due to the heterogeneity of studies: a Rome Foundation working team  
723 literature review. *Gut* *66*, 1075–1082.
- 724 Stasi, C., Bellini, M., Bassotti, G., Blandizzi, C., and Milani, S. (2014). Serotonin receptors  
725 and their role in the pathophysiology and therapy of irritable bowel syndrome. *Tech.*  
726 *Coloproctol.* *18*, 613–621.
- 727 Thijssen, A.Y., Mujagic, Z., Jonkers, D., Ludidi, S., Keszthelyi, D., Hesselink, M.A.,  
728 Clemens, C.H.M., Conchillo, J.M., Kruimel, J.W., and Masclee, A.A.M. (2016). Alterations  
729 in serotonin metabolism in the irritable bowel syndrome. *Aliment. Pharmacol. Ther.* *43*, 272–  
730 282.
- 731 Wei, W., Wang, H.-F., Zhang, Y., Zhang, Y.-L., Niu, B.-Y., and Yao, S.-K. (2020). Altered  
732 metabolism of bile acids correlates with clinical parameters and the gut microbiota in patients  
733 with diarrhea-predominant irritable bowel syndrome. *World J. Gastroenterol.* *26*, 7153–7172.
- 734 Wong, H.L.X., Qin, H., Tsang, S.W., Zuo, X., Che, S., Chow, C.F.W., Li, X., Xiao, H., Zhao,  
735 L., and Huang, T. (2019). Early life stress disrupts intestinal homeostasis via NGF-TrkA  
736 signaling. *Nat. Commun.* *10*, 1–14.
- 737 Xie, Z., and Miller, G.M. (2008).  $\beta$ -phenylethylamine alters monoamine transporter function  
738 via trace amine-associated receptor 1: implication for modulatory roles of trace amines in  
739 brain. *J. Pharmacol. Exp. Ther.* *325*, 617–628.
- 740 Yano, J.M., Yu, K., Donaldson, G.P., Shastri, G.G., Ann, P., Ma, L., Nagler, C.R., Ismagilov,

- 741 R.F., Mazmanian, S.K., and Hsiao, E.Y. (2015). Indigenous bacteria from the gut microbiota  
742 regulate host serotonin biosynthesis. *Cell* *161*, 264–276.
- 743 Young, E.A., Neff, N.H., and Hadjiconstantinou, M. (1993). Evidence for cyclic  
744 AMP-mediated increase of aromatic L-amino acid decarboxylase activity in the striatum  
745 and midbrain. *J. Neurochem.* *60*, 2331–2333.
- 746 Zhao, L., Yang, W., Chen, Y., Huang, F., Lu, L., Lin, C., Huang, T., Ning, Z., Zhai, L., and  
747 Zhong, L.L.D. (2019). A Clostridia-rich microbiota enhances bile acid excretion in diarrhea-  
748 predominant irritable bowel syndrome. *J. Clin. Invest.* *130*.
- 749 Zhao, L., Yang, W., Chen, Y., Huang, F., Lu, L., Lin, C., Huang, T., Ning, Z., Zhai, L., and  
750 Zhong, L.L.D. (2020). A Clostridia-rich microbiota enhances bile acid excretion in diarrhea-  
751 predominant irritable bowel syndrome. *J. Clin. Invest.* *130*, 438–450.
- 752

Graphical abstract

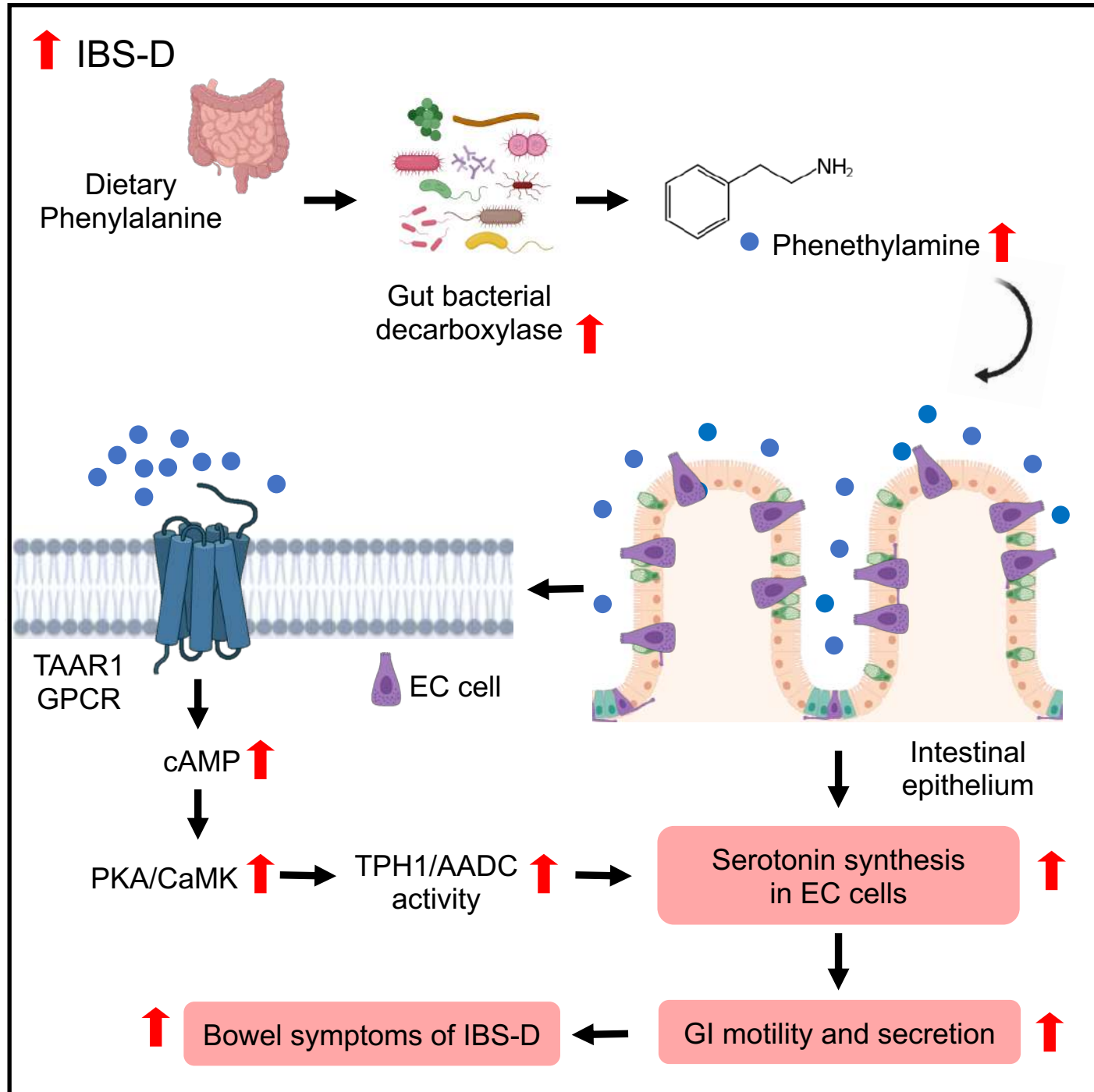


Figure.1

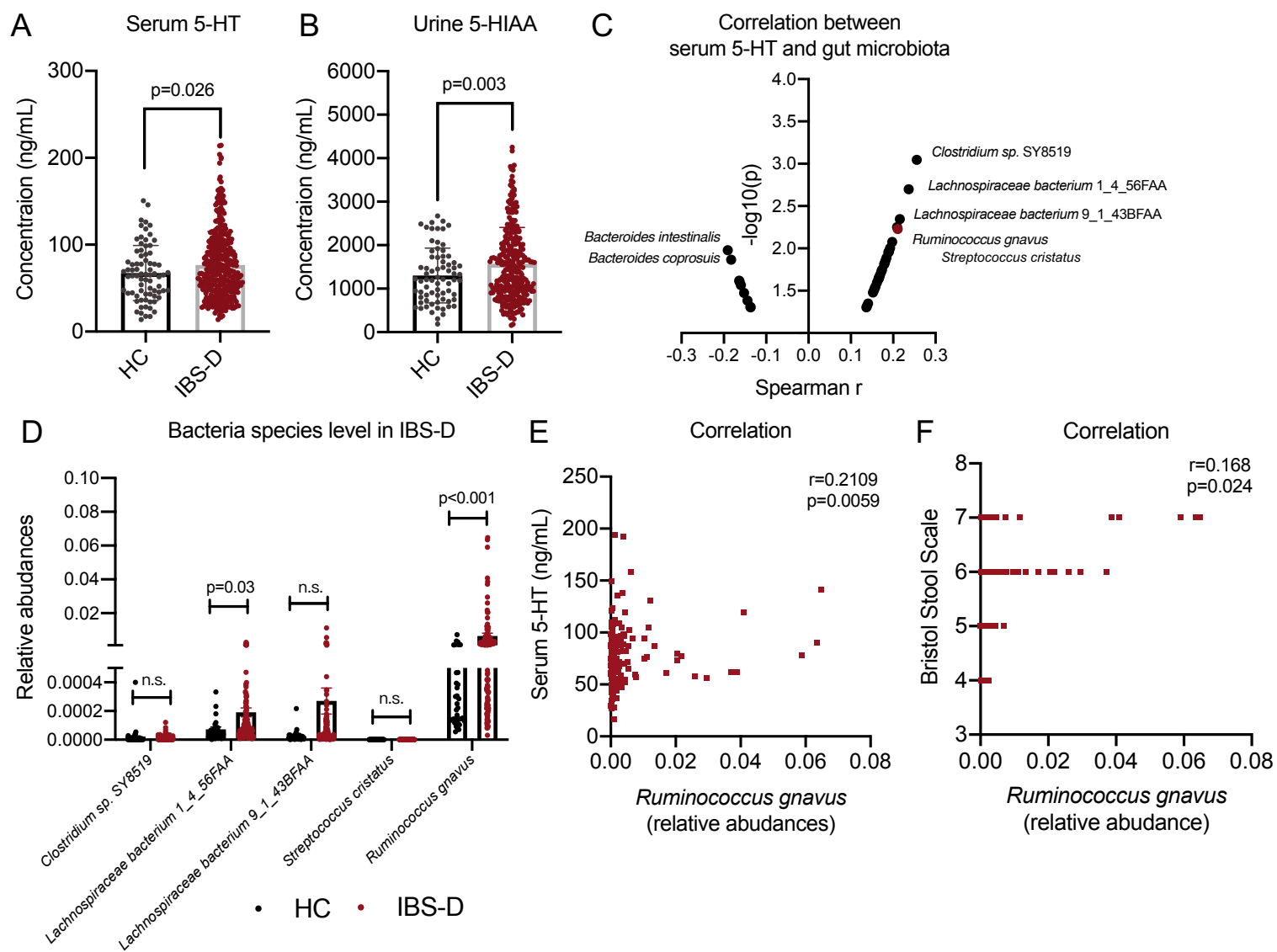




Figure.2

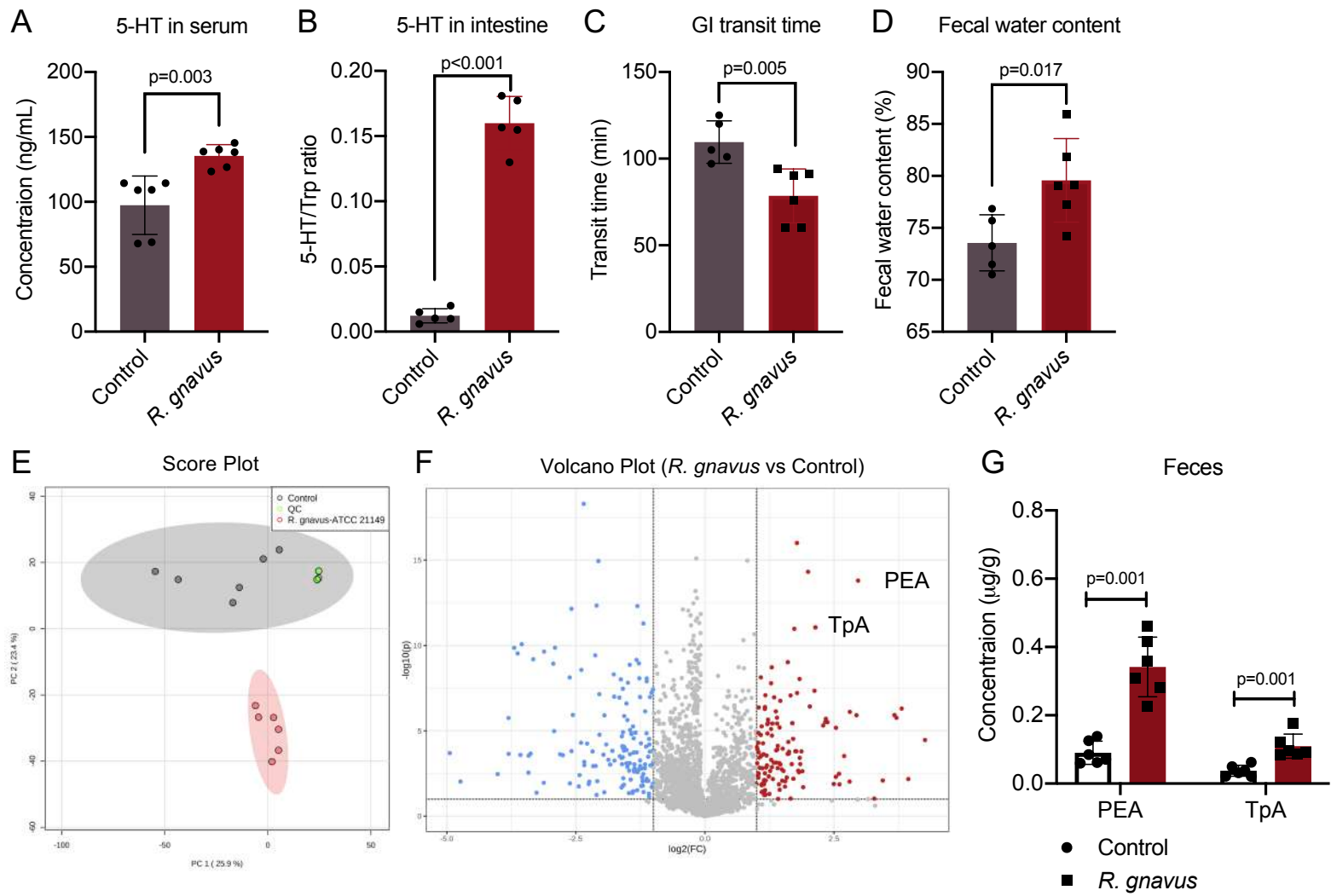


Figure.3

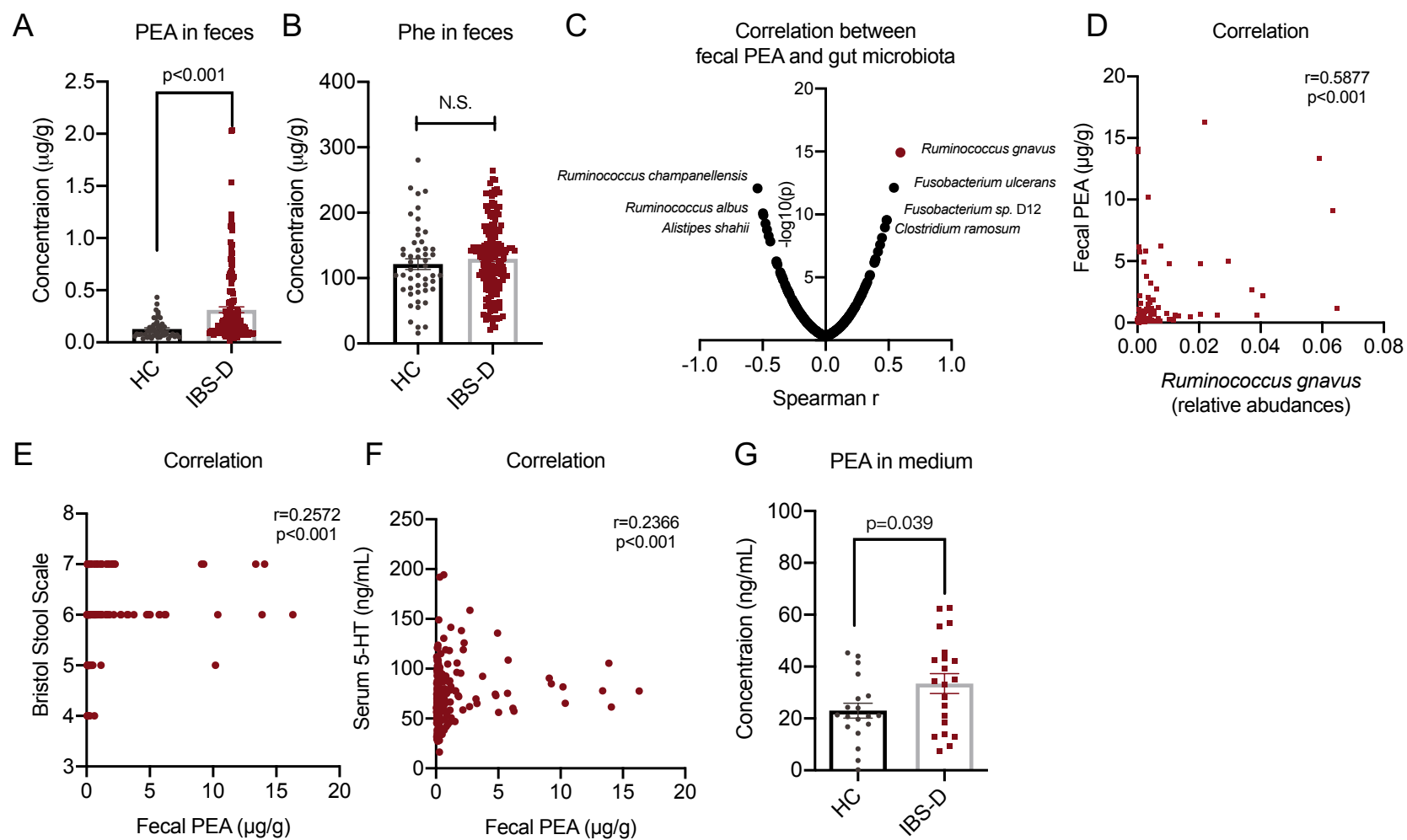


Figure.4

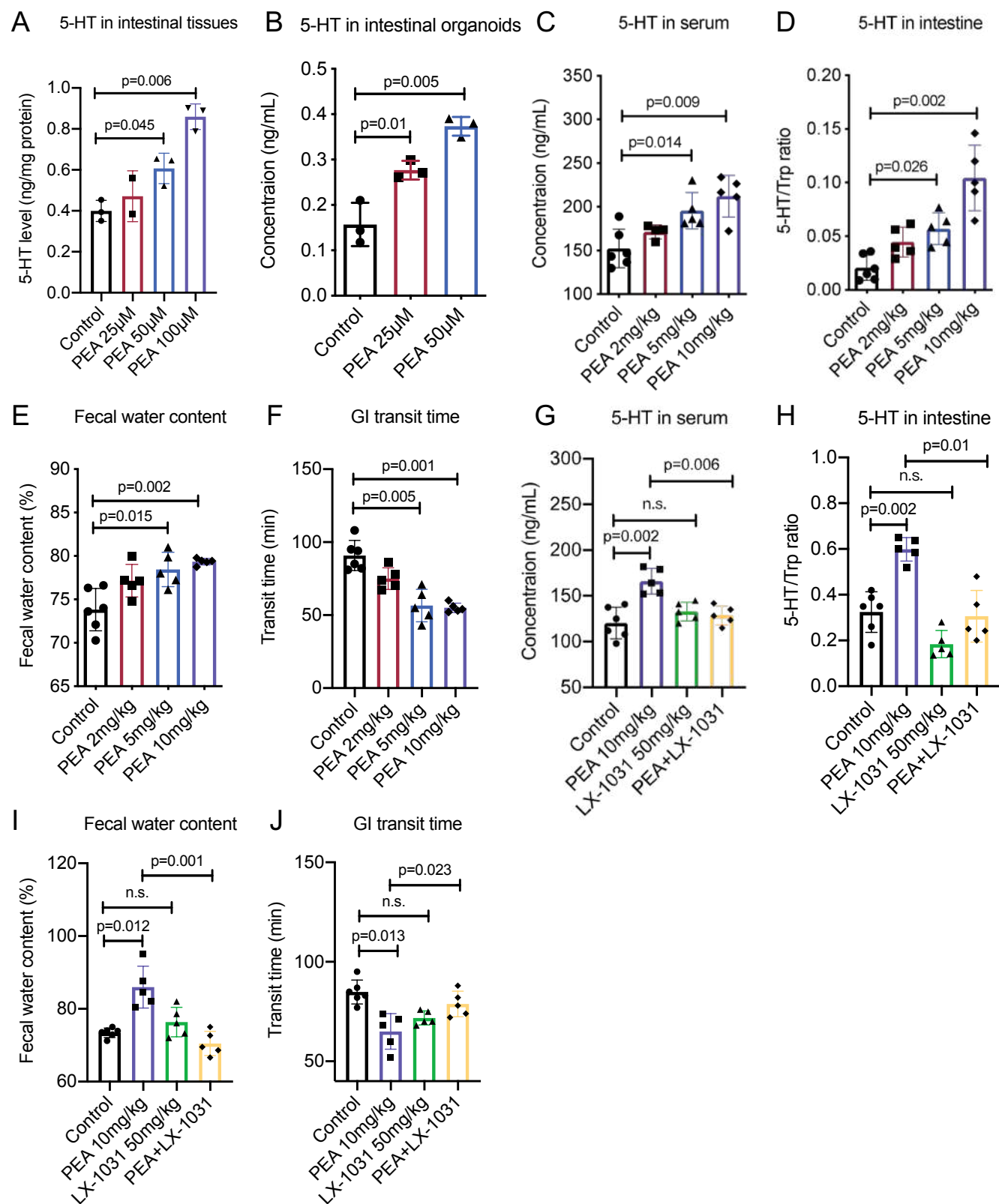


Figure.5

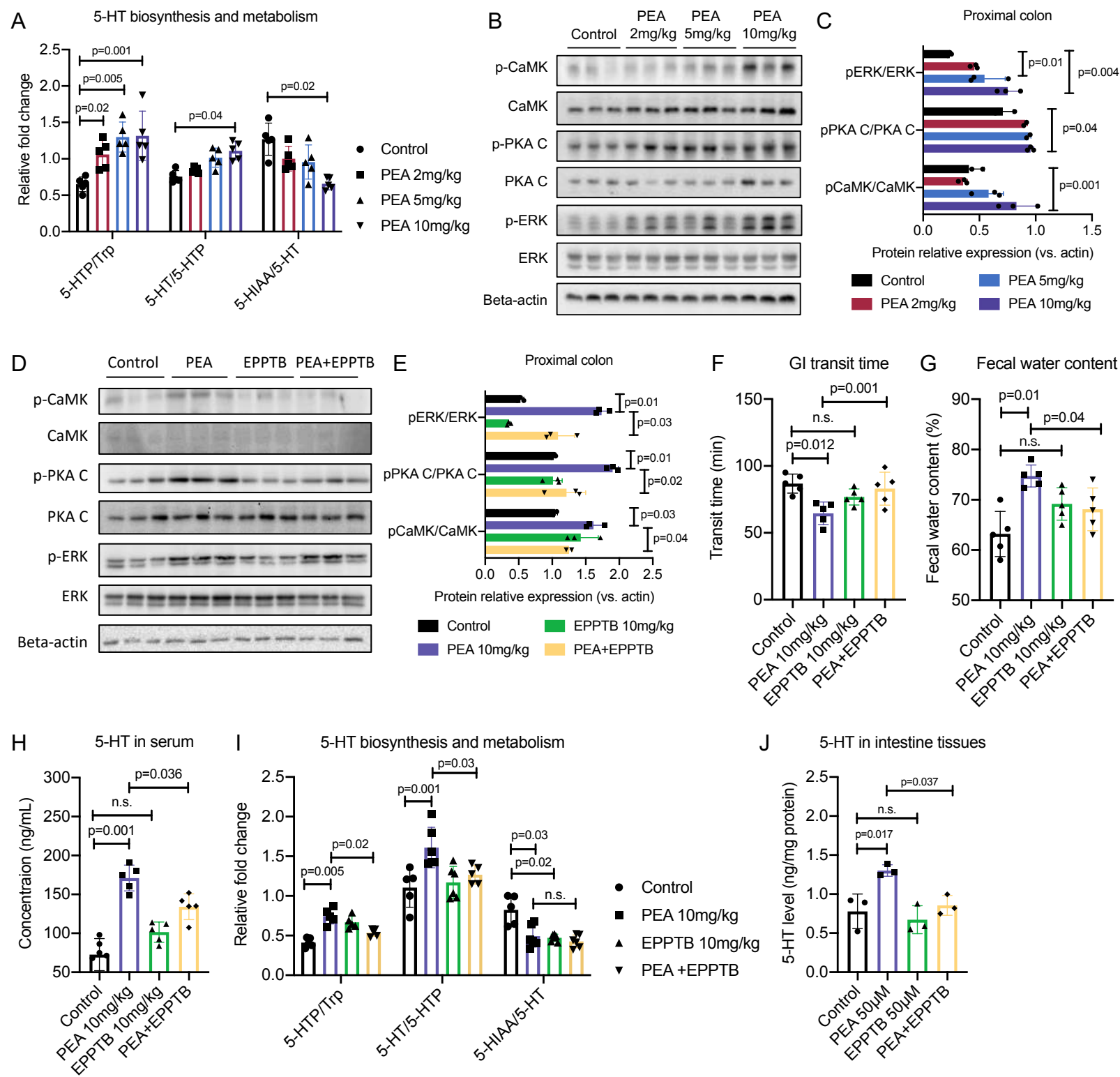


Figure.6

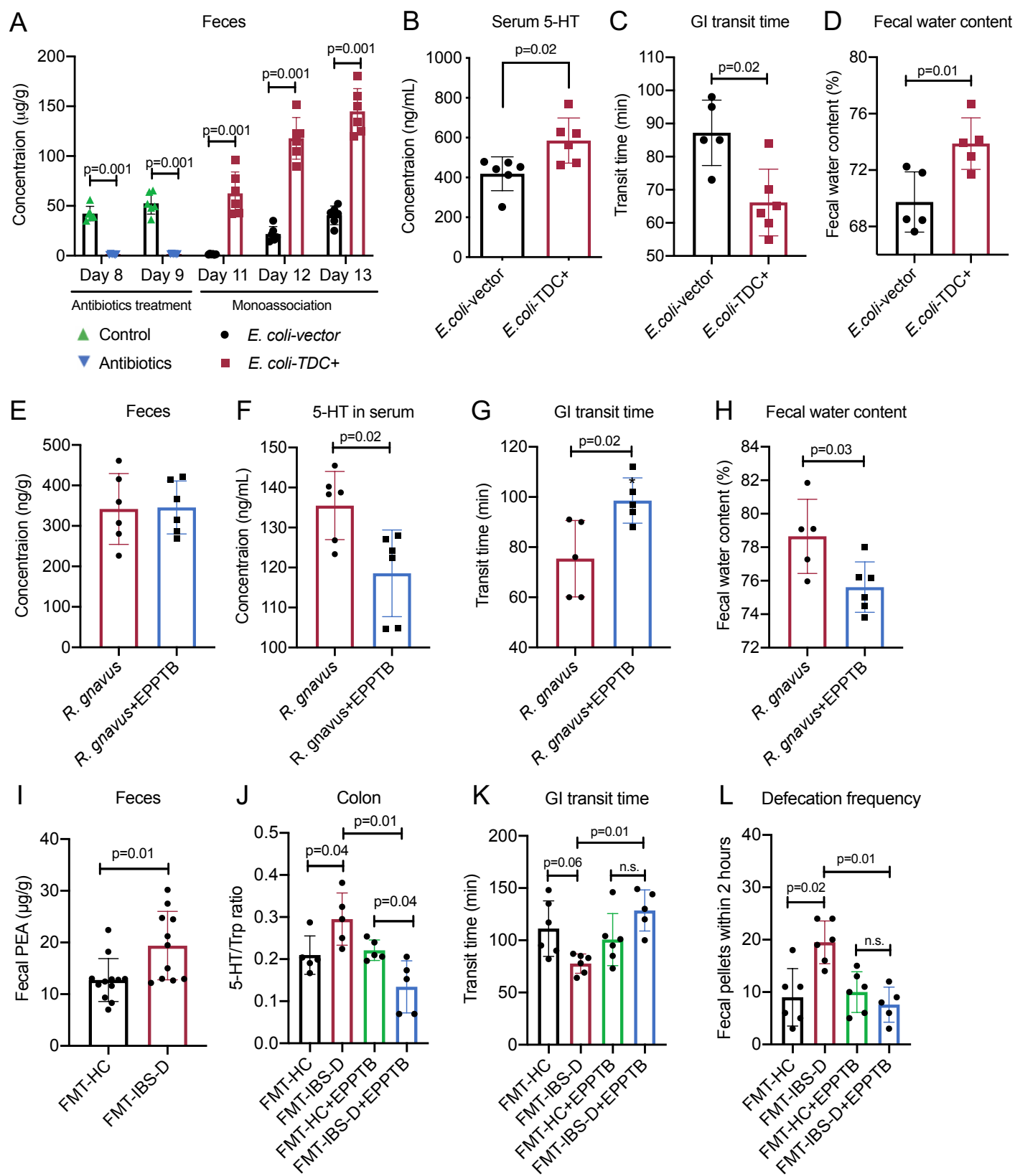
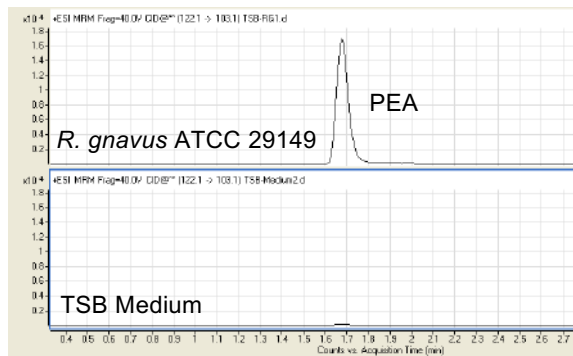


Figure.S1

A LC-MS Chromatogram



B LC-MS Chromatogram

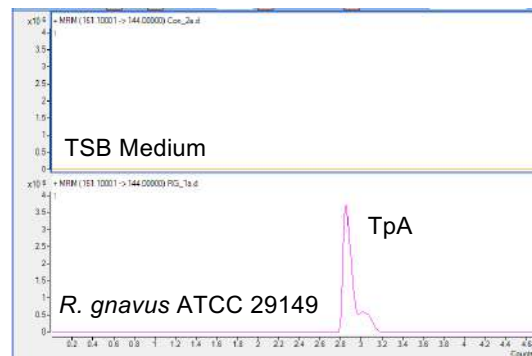


Figure.S2

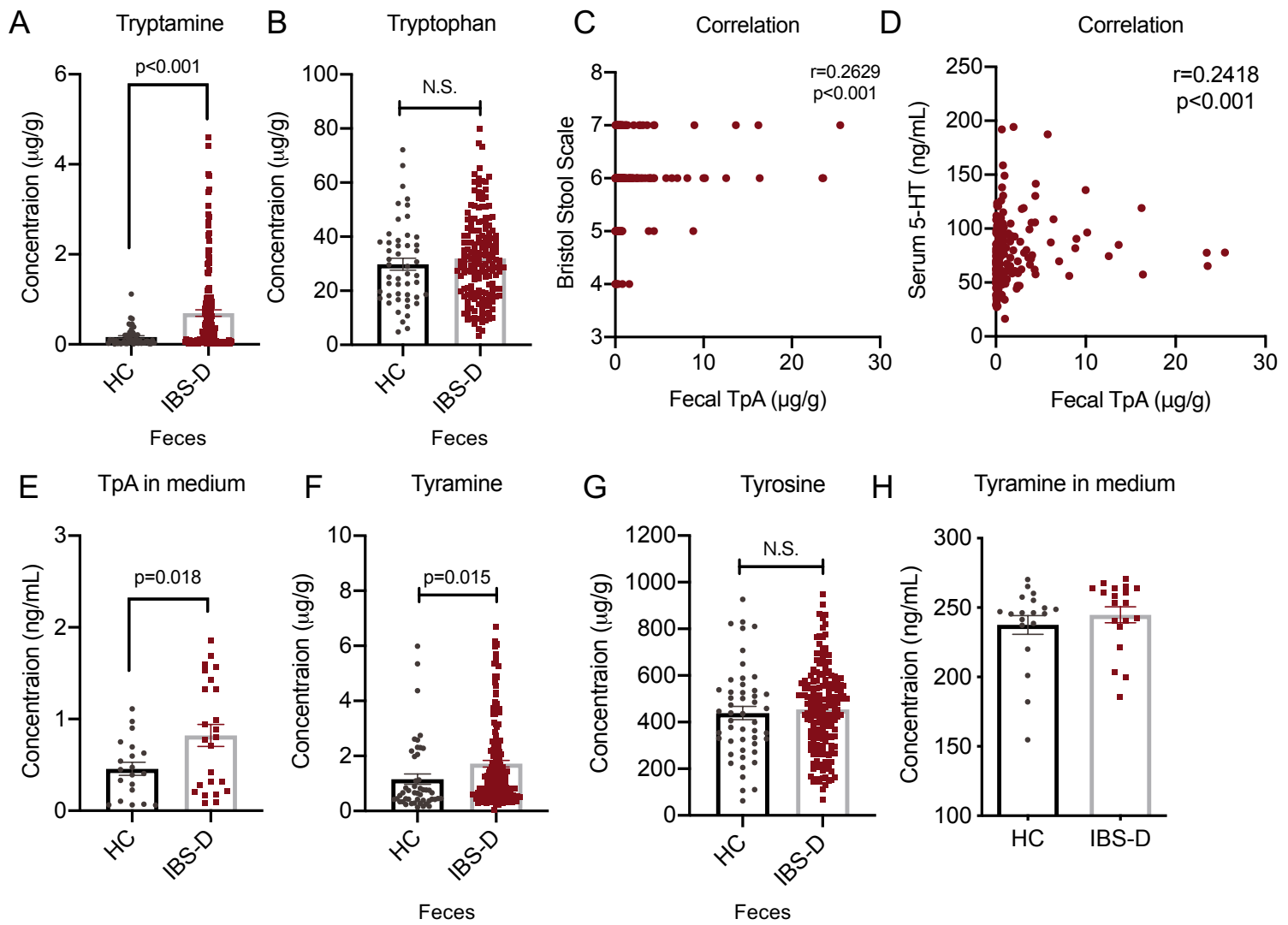


Figure.S3

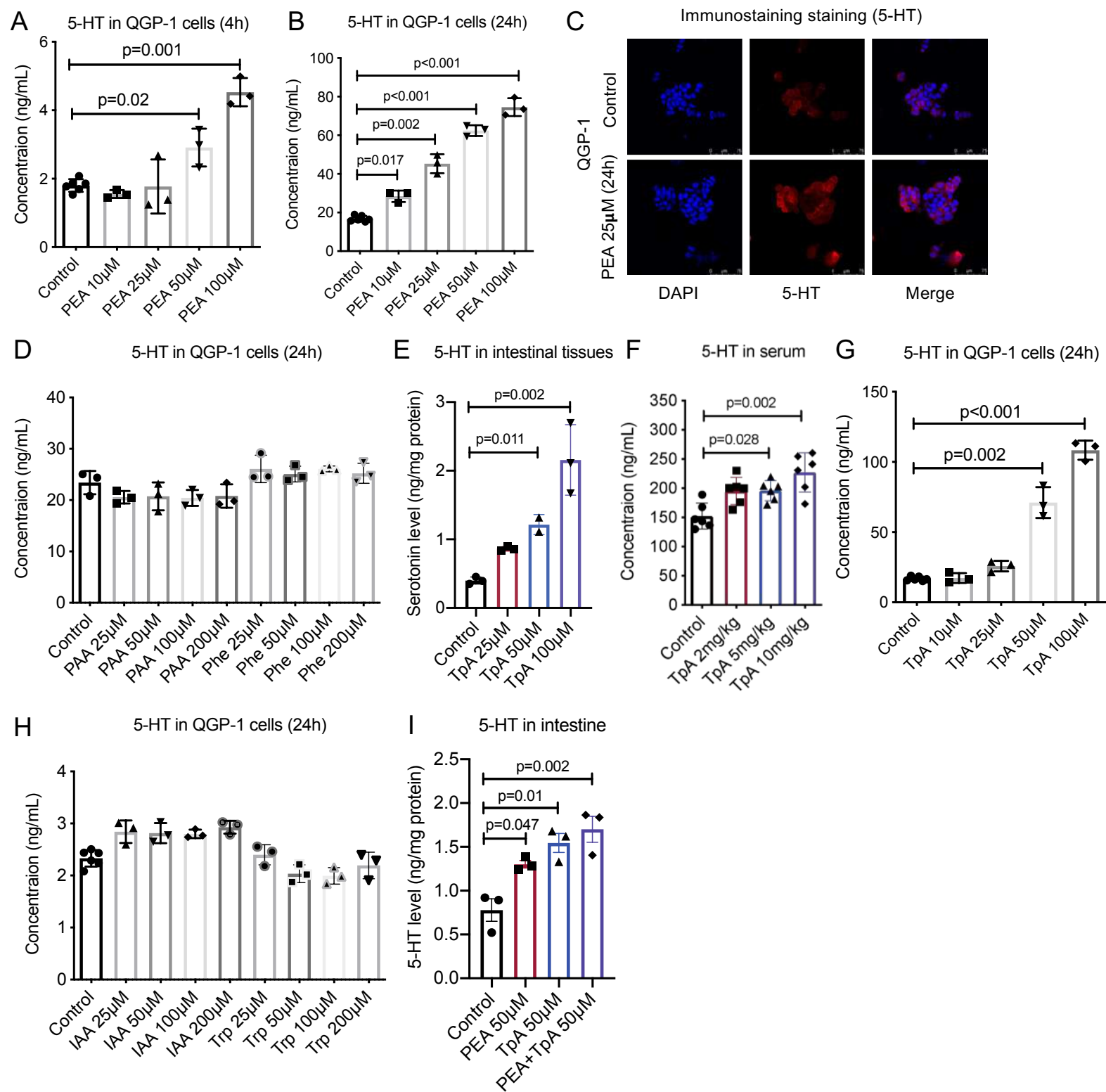




Figure.S4

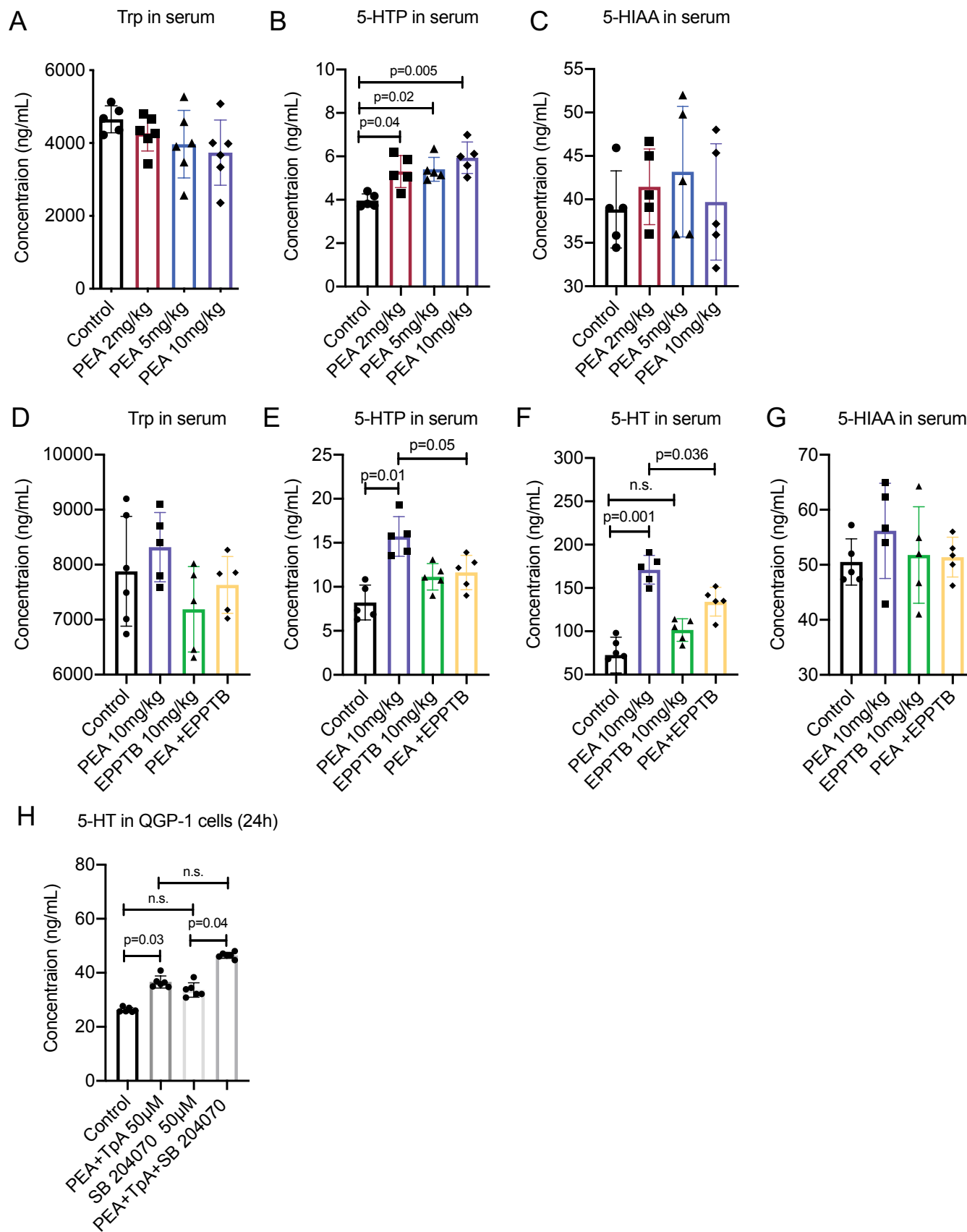
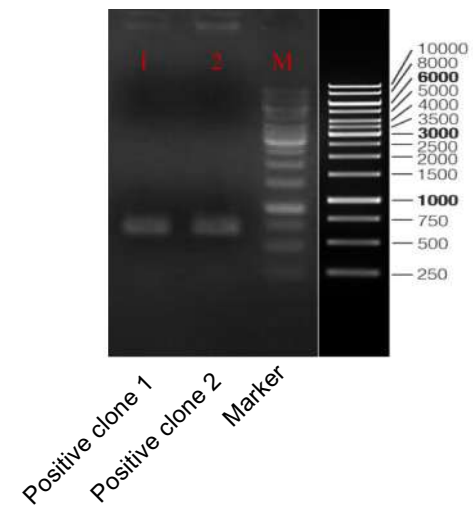
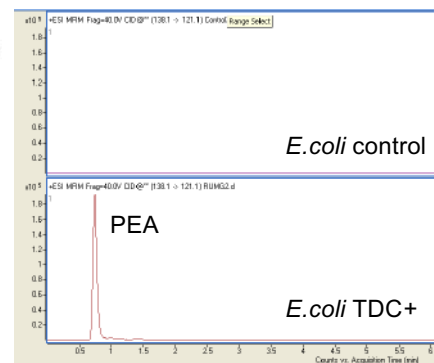


Figure.S5

A PCR electrophoresis



B LC-MS Chromatogram



C LC-MS Chromatogram

